Contrib Mineral Petrol (2009) 158:563–588
DOI 10.1007/s00410-009-0397-2

ORIGINAL PAPER

Adakite-like volcanism of Ecuador: lower crust magmatic evolution and recycling

Massimo Chiaradia · Othmar Müntener · Bernardo Beate · Denis Fontignie

Received: 23 September 2008 / Accepted: 25 February 2009 / Published online: 14 March 2009

Abstract In the Northern Andes of Ecuador, a broad Quaternary volcanic arc with significant across-arc geochemical changes sits upon continental crust consisting of accreted oceanic and continental terranes. Quaternary volcanic centers occur, from west to east, along the Western Cordillera (frontal arc), in the Inter-Andean Depression and along the Eastern Cordillera (main arc), and in the Sub-Andean Zone (back-arc). The adakite-like signatures of the frontal and main arc volcanoes have been interpreted either as the result of slab melting plus subsequent slab melt–mantle interactions or of lower crustal melting, fractional crystallization, and assimilation processes. In this paper, we present petrographic, geochemical, and isotopic (Sr, Nd, Pb) data on dominantly andesitic to dacitic volcanic rocks as well as crustal xenolith and cumulate samples from five volcanic centers (Pululagua, Pichincha, Ilalo, Chacana, Sumaco) forming a NW–SE transect at about 0° latitude and encompassing the frontal (Pululagua, Pichincha), main (Ilalo, Chacana), and back-arc (Sumaco) chains. All rocks display typical subduction-related geochemical signatures, such as Nb and Ta negative anomalies and LILE enrichment. They show a relative depletion of fluid-mobile elements and a general increase in incompatible elements from the front to the back-arc suggesting derivation from progressively lower degrees of partial melting of the mantle wedge induced by decreasing amounts of fluids released from the slab. We observe widespread petrographic evidence of interaction of primary melts with mafic xenoliths as well as with clinopyroxene- and/or amphibole-bearing cumulates and of magma mixing at all frontal and main arc volcanic centers. Within each volcanic center, rocks display correlations between evolution indices and radiogenic isotopes, although absolute variations of radiogenic isotopes are small and their values are overall rather primitive (e.g., $\varepsilon_{Nd} = +1.5$ to $+6$, $^{87}Sr/^{86}Sr = 0.7040$–0.70435). Rare earth element patterns are characterized by variably fractionated light to heavy REE ($La/Yb_N = 5.7$–34) and by the absence of Eu negative anomalies suggesting evolution of these rocks with limited plagioclase fractionation. We interpret the petrographic, geochemical, and isotopic data as indicating open-system evolution at all volcanic centers characterized by fractional crystallization and magma mixing processes at different lower- to mid-crustal levels as well as by assimilation of mafic lower crust and/or its partial melts. Thus, we propose that the adakite-like signatures of Ecuadorian rocks (e.g., high Sr/Y and La/Yb values) are primarily the result of lower- to mid-crustal processing of mantle-derived melts, rather than of slab melts and slab melt–mantle interactions. The isotopic signatures of the least evolved adakite-like rocks of the active and recent volcanoes are the same as those of Tertiary "normal" calc-alkaline magmatic rocks of Ecuador suggesting that the source of the magma did not change

Communicated by T. L. Grove.

Electronic supplementary material The online version of this article (doi:10.1007/s00410-009-0397-2) contains supplementary material, which is available to authorized users.

M. Chiaradia (✉) · D. Fontignie
Department of Mineralogy, University of Geneva, Rue des Maraîchers 13, 1205 Geneva, Switzerland
e-mail: Massimo.Chiaradia@unige.ch

O. Müntener
Institut de Minéralogie et Géochimie, Université de Lausanne, Anthropole, 1015 Lausanne, Switzerland

B. Beate
Escuela Politecnica Nacional, Quito, Ecuador

through time. What changed was the depth of magmatic evolution, probably as a consequence of increased compression induced by the stronger coupling between the subducting and overriding plates associated with subduction of the aseismic Carnegie Ridge.

Keywords Ecuador · Quaternary · Volcanism · Igneous fractionation · Adakite · Radiogenic isotopes

Introduction

The Andean Cordillera is one of the best examples of active continental arc magmatism on Earth. Along-arc variations in crustal thickness and composition as well as in subduction styles produce magmatic rocks that differ in geochemical and isotopic characteristics and indicate that various sources have contributed to their origin (e.g., James 1982; Thorpe et al. 1983; Harmon et al. 1984).

The Northern Andes of Ecuador are particularly interesting because a broad active volcanic arc has developed upon a crust consisting of both oceanic and continental accreted terranes (e.g., Feininger 1987; Litherland et al. 1994), which allows evaluation of magma interaction with different crust types, and because of the occurrence of Quaternary magmatic rocks with adakite-like features (e.g., Bourdon et al. 2003). Adakites were initially defined by Defant and Drummond (1990), following the study of Kay (1978), as magmatic rocks with distinctive geochemical signatures (e.g., Sr $>$ 400 ppm, Y $\leq$ 18 ppm, Yb $\leq$ 1.8 ppm, $La/Yb_N > 10$) derived from melting of subducted oceanic crust and many studies have applied this petrogenetic model to arc rocks with adakite-like signatures (e.g., Kay et al. 1993; Yogodzinski et al. 1995; Stern and Kilian 1996). However, it has also been proposed that the same geochemical signatures of adakites can be formed through other processes, such as partial melting of a mafic lower crust (e.g., Kay et al. 1987; Hildreth and Moorbath 1988; Atherton and Petford 1993) or high-pressure crystallization of hydrous magmas (Müntener et al. 2001; Müntener and Ulmer 2006; Macpherson et al. 2006; Rodríguez et al. 2007; Alonso-Perez et al. 2009). As pointed out by Garrison and Davidson (2003), among others, magmatic rocks with adakite-like signatures can be any rock that has formed from a basaltic protolith under pH_2O–T conditions in which plagioclase is not stable and garnet (and/or amphibole) are stable. The correct interpretation of the genesis of adakite-like rock may have implications for the exploration of porphyry–Cu–Au deposits (adakite-like rocks having been often associated with the latter; e.g., Thieblemont et al. 1997; Kay et al. 1999; Kay and Mpodozis 2001; Cooke et al. 2005) and for the understanding of crustal growth processes (e.g., Kelemen 1995; Martin 1999; Smithies 2000; Kamber et al. 2002; Condie 2005; Martin et al. 2005).

In a series of recent papers (e.g., Bourdon et al. 2002, 2003; Samaniego et al. 2002; Hidalgo et al. 2007; Hoffer et al. 2008), the adakite-like rocks of Ecuador have been considered the result of slab melting, but other works on the same rocks suggest the possible role played by magmatic processes at lower crustal levels (Kilian et al. 1995; Arculus et al. 1999; Monzier et al. 1999; Garrison and Davidson 2003; Chiaradia et al. 2004a; Bryant et al. 2006; Garrison et al. 2006), a petrogenetic process invoked also to explain the geochemical signatures of southern Colombian volcanoes (e.g., Droux and Delaloye 1996; Calvache and Williams 1997).

In this study we report new petrographic, geochemical and isotopic (Pb, Sr, Nd) data of volcanic rocks from a transect across the Ecuadorian arc between latitudes 0°30′N and 0°30′S including Quaternary volcanic centers of the frontal arc (Pululagua, Pichincha), main arc (Chacana and Ilalo), and back-arc (Sumaco) (Fig. 1). Our new data show that, although slab melt metasomatism of the mantle wedge cannot be ruled out, the observed adakite-like signatures of the volcanic rocks of Ecuador are best explained as the result of high-pressure fractionation of mantle-derived melts in the stability field of amphibole ± garnet, accompanied by assimilation of mafic lower crust and/or mixing with its partial melting products.

Geological and geotectonic setting

Ecuador consists of six main physiographic domains (from west to east: Coastal Plain, Western Cordillera, Inter-Andean Depression, Eastern Cordillera, Sub-Andean Zone, Amazon Basin), the four westernmost of which roughly coincide with proposed terranes of both continental and oceanic affinity (Fig. 1a, b). These terranes were accreted to the continental margin (Sub-Andean Zone and Amazon Basin, Fig. 1b) between the Late Jurassic and the Late Cretaceous (Feininger 1987; Megard 1989; Jaillard et al. 1990, 1997; Aspden and Litherland 1992; Litherland et al. 1994; Kerr et al. 1997; Reynaud et al. 1999; Hughes and Pilatasig 2002; Mamberti et al. 2003; Kerr and Tarney 2005; Vallejo et al. 2006). Geophysical (Feininger and Seguin 1983) and geochemical (e.g., Mamberti et al. 2003) data indicate the existence of an oceanic plateau basement in the Coastal Plain and under the Western Cordillera of Ecuador upon which various Late Cretaceous and Tertiary arcs were built. In contrast, the basement underneath the Inter-Andean Depression remains elusive due to the thick Tertiary and Quaternary volcanoclastic cover (a zone of tectonic melange has been proposed by Spikings et al. 2005). The basement of the Eastern Cordillera consists of

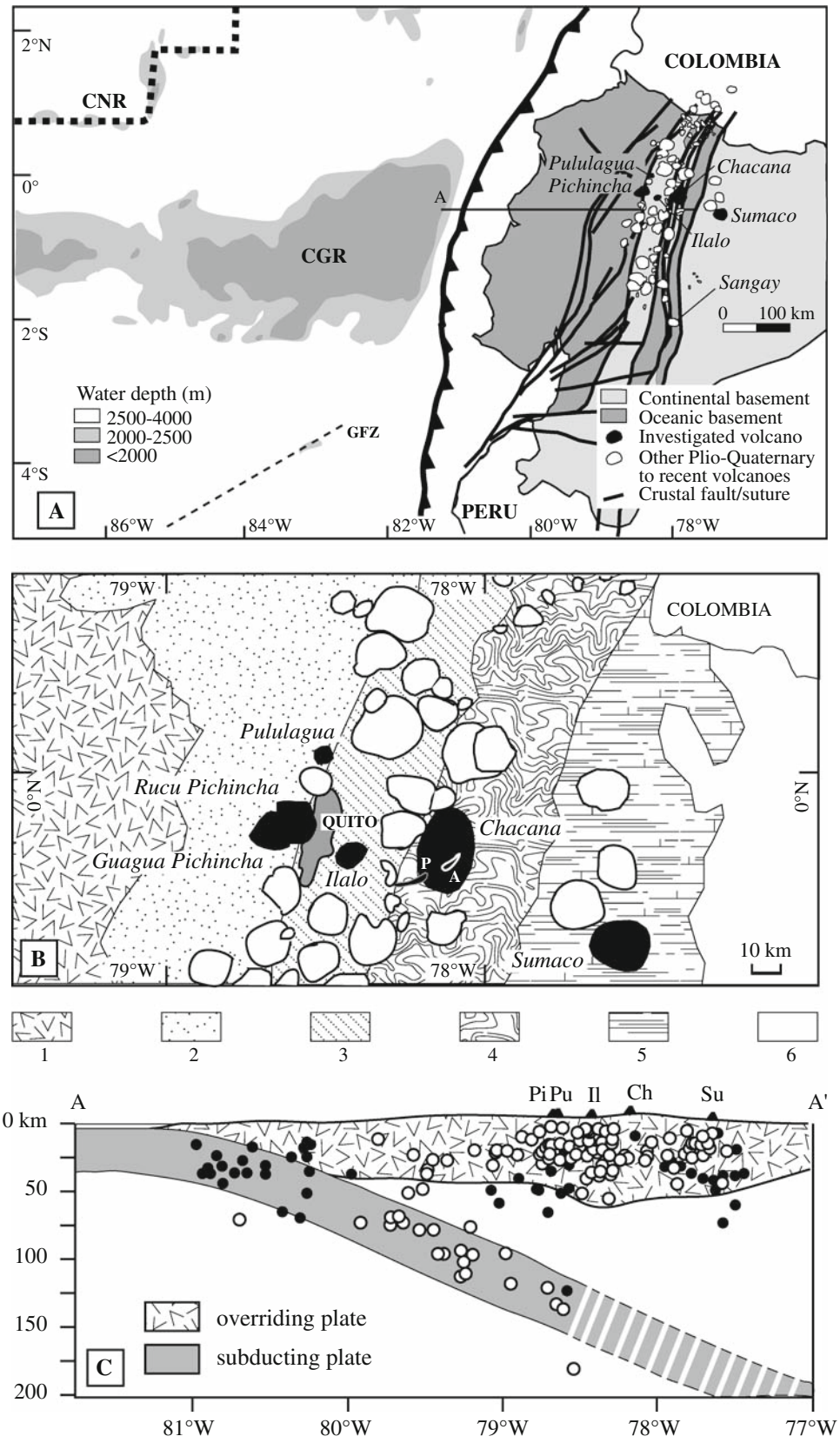

Fig. 1 **a** Geotectonic map of Ecuador with localization of the studied volcanoes (modified after Litherland et al. 1994) and topography of the subducting Carnegie Ridge. **b** Simplified physiographic and geologic map of the study area showing the investigated volcanoes (*in black*) and other Plio-Quaternary volcanic centers (*in white*). Legend: *1* Coastal Plain: Cretaceous oceanic plateaus and overlying island arcs; *2* Western Cordillera: Cretaceous oceanic plateaus and overlying Cretaceous to Tertiary arcs (including Macuchi and Rio Cala arcs); *3* Inter-Andean Depression: Tertiary to Quaternary volcanic and sedimentary cover; *4* Eastern Cordillera: Paleozoic to Jurassic metamorphic and plutonic rocks; *5* Sub-Andean Zone: Proterozoic metamorphic rocks, Jurassic plutonic rocks and overlying Cretaceous sedimentary cover; *6* Amazon Basin. Details within Chacana: *A* Antisanilla flow (1,760 AD); *P* Potrerillos/Papallacta flow (1,773 AD). *C* Cross-section of the Ecuadorian subduction zone, along line *A*–*A′* in Fig. 1b, reconstructed from hypocenters measured by Engdahl et al. (1988) (*black dots*) and Guillier et al. (2001) (*open circles*) (redrawn from Guillier et al. 2001). *Pi* Pichincha, *Pu* Pululagua, *Il* Ilalo, *Ch* Chacana, *Su* Sumaco

metamorphic Paleozoic to Jurassic rocks that would belong to both continental (schists, gneisses, granites) and oceanic (metabasalts) accreted terranes (Aspden and Litherland 1992; Litherland et al. 1994). Recently, however, Pratt et al. (2005) have questioned the allochthonous nature of the Eastern Cordillera terranes. The Sub-Andean Zone consists largely of Jurassic arc plutonic and volcanoclastic rocks and Cretaceous sedimentary cover emplaced within and upon the western margin of the Amazon Craton, which itself consists at depth of Proterozoic metamorphic rocks extending eastwards into the Amazon Basin.

Quaternary volcanism in Ecuador results from the eastward subduction of the 12- to 20-My-year-old Nazca Plate and is restricted to the arc section north of 2°S, Sangay being the southernmost active volcano (Fig. 1a). To the south, magmatic activity continued up to the Late Miocene–Early Pliocene (Beate et al. 2001) and then ceased, due to the onset of the Peruvian flat slab subduction (Barazangi and Isacks 1976). The Quaternary volcanic arc of Ecuador extends over more than 100 km across the Andean chain starting in the Western Cordillera (frontal arc), passing through the Inter-Andean Valley and the Eastern Cordillera (main arc) and ending in the Sub-Andean Zone (back-arc) (Fig. 1b). Such a broad volcanic arc stands in contrast to the narrower volcanic arc immediately to the north, in Colombia, and to the volcanic gap south of 2°S (Fig. 1a). The subduction of the aseismic Carnegie Ridge in coincidence with the Ecuadorian volcanic arc suggests a direct link with such arc broadening.

Guillier et al. (2001) have shown that the Nazca Plate subducting beneath Northern and Central Ecuador has regular dips of 25°–30° down to 150–200 km (Fig. 1c), confirming results of previous investigations by Lonsdale (1978), Pennington (1981) and Prévot et al. (1996). The lack of earthquakes below this depth, roughly coinciding with the onset of the volcanic front at the surface, is a common feature of subduction zones in which <20–My–old oceanic lithosphere is subducting and has been ascribed to the transition from a hydrous seismogenic to an almost anhydrous aseismogenic subducting crust (Hacker et al. 2003). The thickness of the crust, based on gravimetric data (Feininger and Seguin 1983), is 25–30 km beneath the Western Cordillera and more than 50 km under the Eastern Cordillera, then thinning eastwards. Based on the depth of seismic activity, crustal thickness has been estimated to 40–50 km beneath the Western Cordillera and to 50–75 Km beneath the Eastern Cordillera (Guillier et al. 2001; Fig. 1c). Thus, despite their lower mean elevation, the Ecuadorian Andes have a similar crustal thickness to the Central Andes, which has been explained by the higher density of the oceanic material underplated beneath Ecuador (Guillier et al. 2001).

The Carnegie Ridge subduction (Fig. 1a) is causing an increased coupling between the subducted and overriding plate (Gutscher et al. 1999; Sage et al. 2006). Uncertainties exist about the initiation of the Carnegie Ridge subduction, this latter ranging from proposed 1 My (Lonsdale and Klitgord 1978; Gutscher et al. 1999) to 9–15 My ago (Spikings et al. 2001). Pedoja et al. (2006) suggest that the different timing proposed might arise from the arrival of successive discrete segments of the Carnegie Ridge, which at present shows a segmentation into two parts separated by a topographic low (Fig. 1a). This might have caused periodically increased coupling between subducting and overriding plates and consequent compression (e.g., Graindorge et al. 2004; Ego et al. 1996). Villagomez et al. (2002) have suggested that, at latitudes corresponding to those of the investigated transect, the stress regime switched from E–W extensional during the Late Pliocene (which caused the opening of the Inter-Andean Valley) to E–W compressional during the Middle Pleistocene. The onset of compression coincides with or slightly precedes the switch from non-adakitic to adakite-like magmatism recorded at several volcanic centers of northern Ecuador (e.g., Cayambe, Samaniego et al. 2005; Pichincha, Bourdon et al. 2002).

Analytical techniques

In the present study we have investigated 52 lavas, 3 crustal xenoliths and 1 cumulate sample from the volcanic centers of Pululagua ($N = 6$), Guagua and Rucu Pichincha ($N = 13$), Ilalo ($N = 4$), Chacana ($N = 19$), and Sumaco ($N = 14$). For discussion, we have added the analyses of four samples of Pululagua, one of Ilalo, three of Chacana and three of Sumaco previously analyzed by Bryant et al. (2006). Details of the analytical techniques used are available in the Electronic Supplementary Appendix.

Results

Geology and petrography of the volcanoes

Pululagua and Pichincha (frontal arc)

Pululagua and Pichincha are two volcanic centers situated in the frontal part of the arc about 30 km apart (Fig. 1b). They sit, respectively, above the accreted Cretaceous Pallatanga oceanic plateau and Late Cretaceous mafic submarine volcanic and volcanosedimentary rocks of the Rio Cala island arc grown on top of the Pallatanga terrane (BGS and CODIGEM 1999, 2001; Vallejo 2007). Pululagua, situated 15 km NNE of Quito, is a 3-km-wide caldera partially filled by dacitic lava domes. Pre-caldera lava domes occur along a roughly N–S line east of the caldera rim. Large explosive eruptions and associated pyroclastic flows took place during

the late Pleistocene and Holocene. Eruptions between 2,650 and 2,450 years ago resulted in the formation of the caldera and were followed by the extrusion of post-caldera lava domes about 1,670 years ago (Global Volcanism Program, http://www.volcano.si.edu/). Pululagua eruptive products are andesitic to dacitic in composition (SiO_2 = 61.3–65.4 wt%, Supplementary Table). They contain amphibole, plagioclase and rare pyroxene phenocrysts, as well as apatite microphenocrysts (up to 200 μm long). Amphibole is often transformed at the rims into a fine-grained association of pyroxene, plagioclase and Fe-oxides (opacite, Fig. 2a). These textures are usually attributed to amphibole–melt reaction during decompression (e.g., Rutherford and Hill 1993). Amphibole is optically zoned, with sub-rounded cores overgrown by one or more outer zones (Fig. 2a). Plagioclase phenocrysts have rounded cores with concentric, convolute or patchy zoning, which are overgrown by thick mantles with concentric zoning. Both plagioclase cores and rims occasionally include amphibole. Pululagua lavas contain mafic granulite xenoliths (consisting of plagioclase, pyroxene and symplectitic Fe-oxides) a few millimeters in size as well as xenoliths of andesitic lavas (probably from the Late Cretaceous Natividad Unit, which constitutes the local substratum), ranging from a few millimeters to several centimeters in size.

Guagua Pichincha and the older, Pleistocene, Rucu Pichincha stratovolcanoes are situated immediately to the west of Quito (Fig. 1b). A lava dome occurs at the head of a 6-km-wide caldera, which is about 50,000 years old. Late Pleistocene and Holocene (also historical) explosive eruptions consisted of pyroclastic flows accompanied by periodic growth and destruction of the lava dome (Global Volcanism Program, http://www.volcano.si.edu/). Guagua Pichincha lavas are andesites (SiO_2 = 61.3–62.8 wt%, Supplementary Table) and contain amphibole, plagioclase and clinopyroxene phenocrysts. Large poikilitic amphibole phenocrysts host inclusions of plagioclase, apatite and quartz marking the limit between adjacent growth zones. Amphibole (plus Fe-oxides) may also form an optically continuous thick rim (several hundreds of micrometers) around clinopyroxene phenocrysts. Guagua Pichincha lavas contain holocrystalline cumulate enclaves consisting of amphibole, plagioclase, and orthopyroxene. Rucu Pichincha lavas are andesitic in composition (SiO_2 = 59.2–63.0 wt%, Supplementary Table) and contain orthopyroxene, clinopyroxene, and plagioclase phenocrysts with sporadic amphibole. Clino- and ortho-pyroxene display disequilibrium textures, with rounded cores surrounded by Mg-rich rims (inverse zoning, Fig. 2b). Plagioclase always displays complex zoned patterns, characterized by resorption and overgrowths of Ca-rich rims (inverse zoning) as well as by sieve textures (Fig. 2c). Pichincha lavas display mingling textures, with the host lavas containing centimeter-sized enclaves consisting of amphibole, plagioclase, orthopyroxene, and olivine phenocrysts in a matrix of tiny plagioclase and amphibole microlaths (<200 μm). These enclaves may be dismembered and mixed almost completely within the host lava, their relic presence being highlighted by the systematic occurrence of patchy zones enriched in plagioclase microlaths within the host lava. Pichincha volcanic rocks contain abundant mafic granulite xenoliths (Fig. 2d, e) and gabbroic cumulates (Fig. 2e), both consisting of orthopyroxene, clinopyroxene, plagioclase, magnetite ± olivine, as well as frequent pyroxene glomerocrysts. The mafic granulite xenoliths, different from cumulates, have an equigranular mosaic texture and display a planar anisotropy highlighted by a rough alternation between pyroxene and plagioclase layers. They have few tens of micrometer thick reaction rims at the contact with the host lava, consisting of glass and sieve-textured plagioclase. The very low incompatible element concentrations of one of these xenoliths (sample E05130a, Supplementary Table) might reveal a restitic character. Ca-rich plagioclase–pyroxene–wollastonite xenoliths (sample E05011, Supplementary Table), with $\varepsilon_{Nd} = -0.74$, and non-radiogenic Pb isotopic composition ($^{206}Pb/^{204}Pb = 18.607$), also occur in lavas of the Pichincha volcanic complex. The holocrystalline texture and large crystal size of these xenoliths indicate that they are either fragments of a high-grade metamorphic basement or that they resided in contact with the host magma long enough to develop their high-grade metamorphic assemblage.

Ilalo and Chacana (main arc)

Ilalo and Chacana are two volcanic edifices of the main volcanic belt of the arc (Fig. 1b). Ilalo, situated about 10 km east of Quito in the Inter-Andean Depression, is an eroded volcano with a small caldera on the western side, which last erupted ~1.6 My ago. Products of this volcano are basaltic andesites to andesites (54.6 wt% < SiO_2 < 57.3 wt%, Supplementary Table) with phenocrysts of zoned pyroxene, olivine (surrounded by a pyroxene rim) and plagioclase in a highly crystalline matrix of pyroxene and plagioclase microlaths (<200 μm). Plagioclase phenocrysts have rounded patchy or convolute cores overgrown by rims of concentrically zoned plagioclase. Ilalo lavas contain abundant pyroxene glomerocrysts and display also mingling textures between intermediate and mafic magmas.

Chacana is an eroded, Pliocene–Holocene caldera complex forming one of the largest rhyolitic centers of the northern Andes (32 km in the N–S direction and 18–24 km in the E–W direction: Global Volcanism Program, http://www.volcano.si.edu/). It is located in the Eastern Cordillera (Fig. 1b) upon the basement of the Loja continental terrane (Paleozoic gneisses and schists as well as Triassic granites) and of the Alao island arc terrane

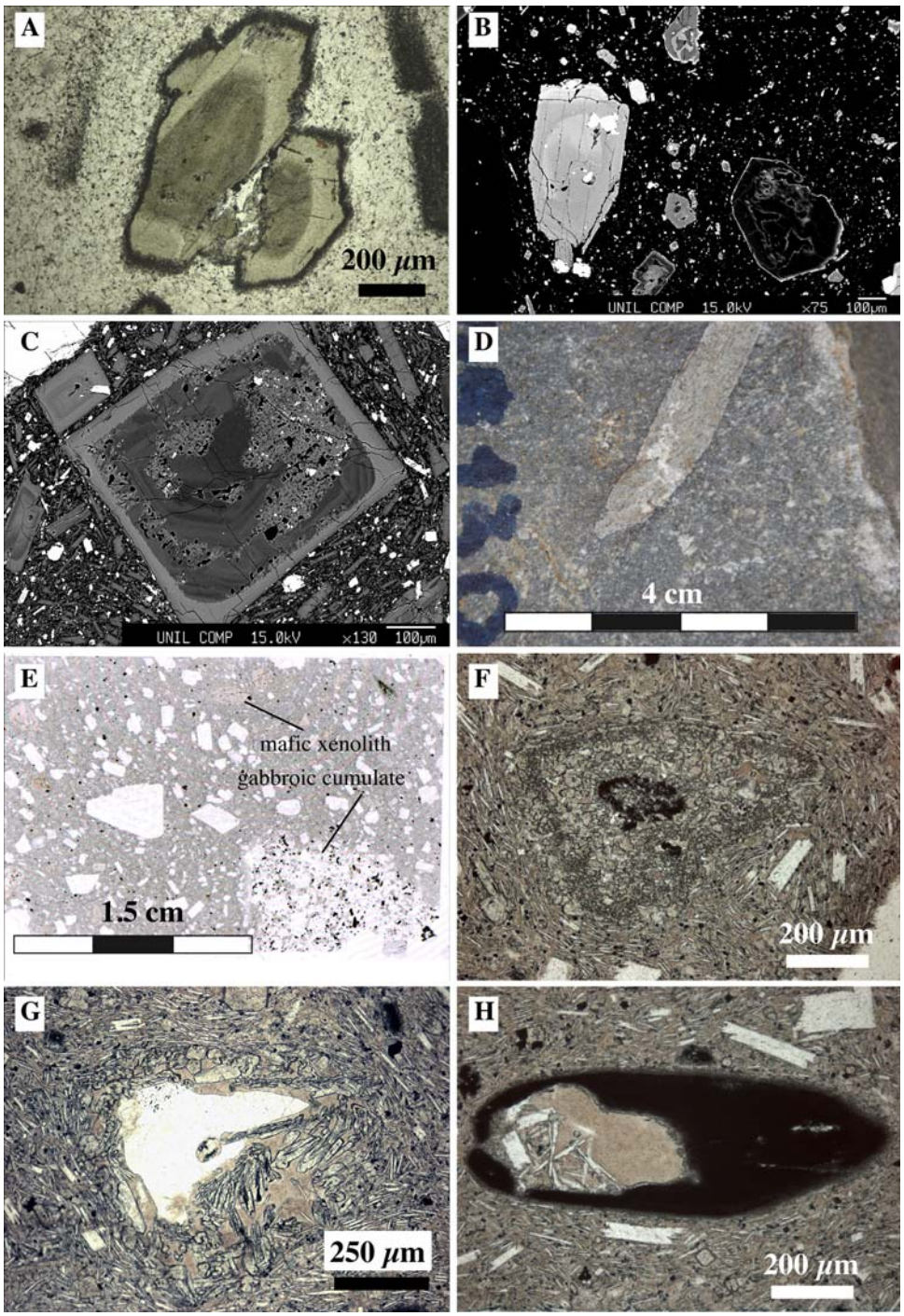

Fig. 2 Microphotographs of volcanic rock samples from the studied volcanoes: **a** Concentrically zoned amphiboles with opacite rims (Pululagua volcano: sample E05003; transmitted light microscope image, parallel nicols); **b** rounded cores in zoned clinopyroxene (*left side*) and orthopyroxene (*bottom*) with reverse zoning (Pichincha volcano: sample E05015; BSE image); **c** plagioclase phenocryst with rounded sieve-textured core overgrown by a Ca-richer rim (Pichincha volcano: sample E05015; BSE image); **d** mafic granulite xenolith in andesitic lava (Pichincha volcano: sample E05130; photograph of rock hand sample); **e** pyroxene glomerocrysts (*dark spots*) and gabbroic cumulate (*bottom right*) in lava (Pichincha volcano: sample E05015; thin section scan image); **f** sieve-textured pyroxene (Chacana volcano: sample E05035; transmitted light microscope image, parallel nicols); **g** quartz xenocryst with glass and clinopyroxene zoned corona (Chacana volcano: sample E05035; transmitted light microscope image, parallel nicols); **h** opacitized amphibole with glassy core (Chacana volcano: sample E05035; transmitted light microscope image, parallel nicols)

(Jurassic meta-basalts) (Aspden and Litherland 1992; Aspden et al. 1992; Litherland et al. 1994; Noble et al. 1997). Chacana was constructed from at least three cycles of andesitic-to-rhyolitic volcanism. Between 30 and 21 ky ago, dacitic flows erupted from caldera-floor fissures, and numerous lava domes were formed within the caldera (Global Volcanism Program, http://www.volcano.si.edu/). During the Holocene, frequent explosive eruptions occurred and historical lava flows (Potrerillos/Papallacta and Antisanilla) are documented during the eighteenth century (Fig. 1b; Supplementary Table). We have investigated lavas from the last 40 ky (Young Chacana), from between 100 and 200 ky (Old Chacana), and older than 0.85 Ma (i.e., pre-caldera, hereafter named pre-Chacana).

Young Chacana andesitic lavas contain plagioclase and pyroxene phenocrysts. Plagioclase displays sieve textures on the outer part of the phenocrysts, which is in turn overgrown by "equilibrium" plagioclase. In some lava

samples (e.g., E05035), pyroxene displays sieve textures identical to those of plagioclase (Fig. 2f). Amphibole, quartz and olivine are important constituents in some samples (e.g., E05032 and E05035), where plagioclase phenocrysts are rare. In these samples, quartz is xenocrystic as indicated by its disequilibrium textures with respect to the host lavas. In fact, embayed quartz xenocrysts coexist with olivine phenocrysts and are surrounded by a corona of glass (Fig. 2g), which is in turn crowned by acicular clinopyroxene aggregates crystallized inward and perpendicular to the contact of the former xenocrysts with the lava (see also Sato 1975). In many cases, the former quartz or other (?) xenocrysts are completely melted and only glass is visible with acicular clinopyroxene crystallized from the rim inward. Quartz xenocrysts could belong to a quartz-bearing felsic magma that was mixed with a more mafic magma (see also Stimac and Pearce 1992; Mashima 2004) or to partially assimilated crustal rocks. Amphibole is variably replaced by a fine aggregate of oxides or by the association pyroxene, plagioclase, magnetite. Glassy cores of amphibole phenocrysts surrounded by an opacite rim have also been observed (Fig. 2h).

Sumaco (back-arc)

Sumaco is the volcano situated farthest from the trench, in the back-arc, sitting in the Sub-Andean Zone (Fig. 1b). Its deep basement consists of high-grade metamorphic rocks of Proterozoic age (Litherland et al. 1994) overlain by Cretaceous sediments. The Sub-Andean zone also hosts Jurassic arc batholiths a few tens of kilometers west of Sumaco. Sumaco is a stratovolcano consisting of SiO_2-undersaturated absarokitic to shoshonitic volcanic and volcanoclastic products. The most primitive samples (SiO_2 = 43–50 wt%, Supplementary Table) have large sector zoned clinopyroxene, haüyne, and amphibole phenocrysts in a matrix of glass and microlithic clinopyroxene and plagioclase. Plagioclase phenocrysts were only found in more evolved samples ($SiO_2 \sim 54$ wt%) where they show oscillatory concentric zoning and more rarely have corroded cores with convoluted zoning overgrown by oscillatory-zoned plagioclase. An historical eruption has been inferred in the eighteenth or early-nineteenth century on the basis of changes in crater morphology (Global Volcanism Program, http://www.volcano.si.edu/).

Geochemistry

Frontal and main arc volcanoes (Pululagua, Pichincha, Ilalo, Chacana)

Investigated rocks of the frontal and main arc volcanic centers range in composition from basaltic andesite to rhyolite (Fig. 3a). Rocks within each volcanic center define similar trends in several major and trace element correlation diagrams (Figs. 3, 4) although some notable differences occur. Samples from Ilalo do not always define clear trends, due to their limited number.

Volcanic products of each frontal and main arc volcanic center are characterized by decreasing Fe_2O_3, MgO, CaO, Ni, and V (as well as, not shown, TiO_2 and Sc) with increasing SiO_2 (Figs. 3, 4) probably due to fractionation of clinopyroxene, olivine and magnetite. Increasing Na_2O and Al_2O_3 with increasing SiO_2 suggest limited plagioclase fractionation at Pululagua and Young Chacana, whereas Pichincha rocks do not show clear trends of Na_2O and Al_2O_3 variations with SiO_2, and Old Chacana and pre-Chacana rocks are characterized by decreasing Al_2O_3 with increasing SiO_2 suggesting abundant plagioclase fractionation (Fig. 3b, c). Petrographic and isotopic data (see later) show, however, that fractional crystallization is not the only responsible for the chemical differentiation of these rocks and that open-system processes have operated as well.

All frontal and main arc centers (except Pululagua) display a significant increase of K_2O and Rb with SiO_2 (Figs. 3, 4). Also Th (and U) contents correlate positively with SiO_2 at Pichincha and Young Chacana (Fig. 4), but remain consistently low at Pululagua, similar to K_2O and Rb. Sr contents of Pululagua, Pichincha and Young Chacana generally correlate positively or, at least, do not decrease with SiO_2, again indicating limited plagioclase fractionation (Fig. 4).

Primitive mantle-normalized spidergrams (Fig. 5a, b) show that rocks of all frontal and main arc volcanic centers have variable LILE enrichment and Nb and Ta (as well as Ti) negative anomalies, a typical subduction-related fingerprint. Rocks of the frontal and main arc volcanic centers display a range of incompatible element enrichment that correlate positively with increasing distance of the volcanic center from the trench (i.e., Pululagua $\sim$ Pichincha $<$ Ilalo $<$ Chacana: Fig. 5).

Excluding Old Chacana and pre-Chacana, REE plots of the frontal and main arc volcanic rocks lack Eu negative anomalies and display variable LREE enrichment over HREE with some fractionation between MREE and HREE (Fig. 5c). Average LREE contents and La/Yb_N generally increase from Pululagua ($La/Yb_N \sim 5.7$) through Pichincha ($La/Yb_N \sim 8.13$) to Chacana ($La/Yb_N \sim 17.52$) following the same tendency of incompatible element enrichment in primitive mantle-normalized spidergrams, whereas average HREE values remain constant at all frontal and main arc centers (Fig. 5). This LREE enrichment again correlates with increasing distance of the volcano from the trench. MREE fractionation with respect to HREE (a potential indicator of amphibole vs. garnet

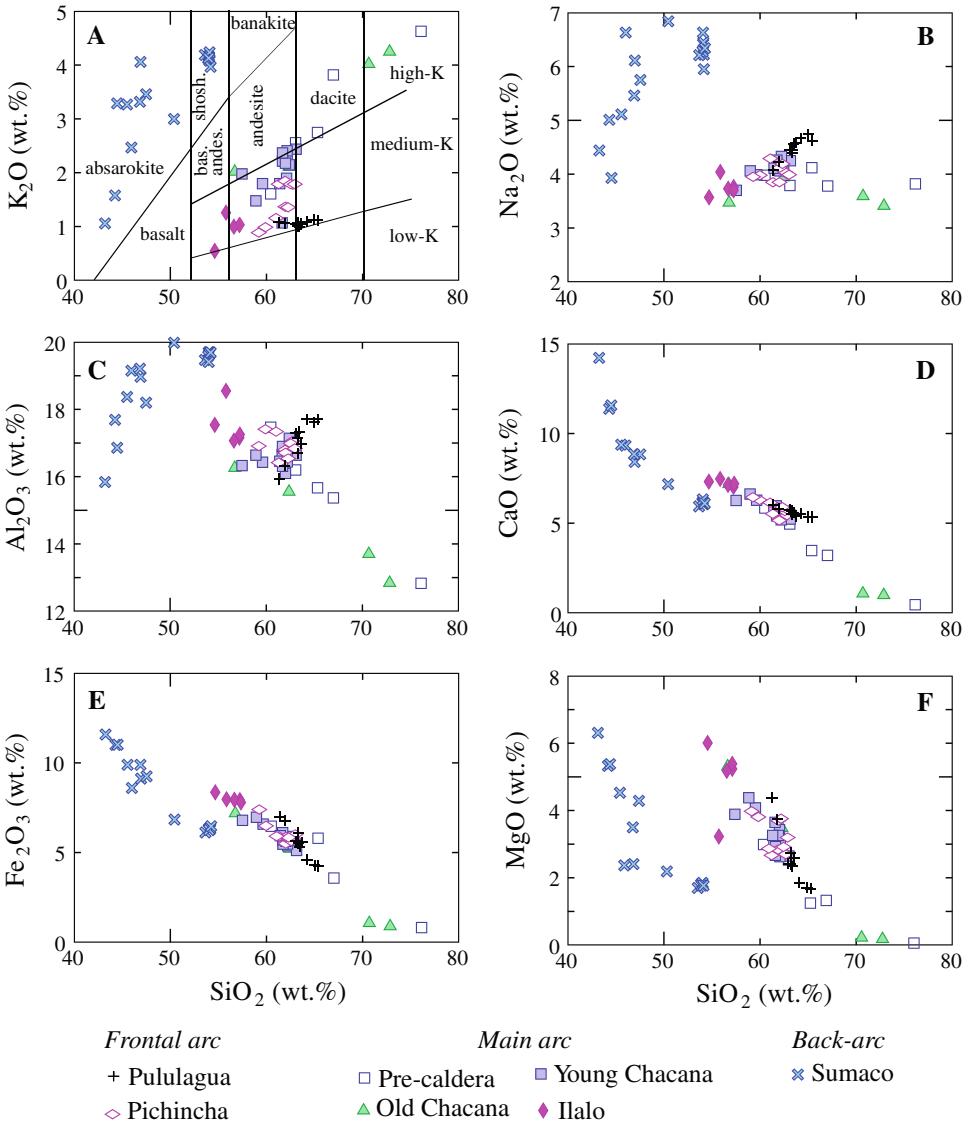

Fig. 3 Major element variations in rocks of the studied volcanoes. The classification scheme of Fig. 3a is from Peccerillo and Taylor (1976)

fractionation) is similar for Pululagua and Pichincha ($Gd/Yb_N \sim 1.9$) and increases at Young Chacana ($Dy/Lu_N \sim 2.6$). All the above features suggest that these rocks originated/evolved for at least part of their history outside the stability field of plagioclase and within the stability field of clinopyroxene, amphibole ± garnet (some garnet fractionation is required in order to explain the MREE/HREE fractionation, see later section on modeling). Old Chacana and pre-Chacana rocks are characterized by variable MREE/HREE fractionation ($Gd/Yb_N \sim 1.9$ for Old Chacana and 1.6 for pre-Chacana) and more or less marked negative Eu anomalies, suggesting prolonged evolution in the stability field of plagioclase (Fig. 5d).

Volcanic rocks of the frontal and main arc plot towards the lower end of the adakite field in the Sr/Y versus Y diagram (Fig. 6a), close to the boundary with the "normal" arc lavas field, but except Young Chacana samples they plot within the "normal" arc rocks field in the La/Yb versus Yb plot (Fig. 6b). Excluding rocks of pre-Chacana, Old Chacana and Ilalo, which do not define clear trends because of the small number of samples, Sr/Y and La/Yb values tend to increase with SiO_2 (and decrease with Ni: not shown) at all frontal and main arc volcanic centers (Fig. 6c, d). The La/Gd ratio increases consistently with SiO_2 at Pululagua, Pichincha and Young Chacana, whereas the Gd/Yb ratio shows a positive correlation with SiO_2 at Young Chacana (Fig. 6e, f). The Nb/Ta ratio is negatively correlated with SiO_2 at all frontal and main arc volcanoes, except Ilalo ($R = 0.87$ at Young Chacana, 0.86 at Pichincha, 0.77 at Pululagua and 0.87 for the three combined centers; Fig. 6g, h), with Nb/Ta values ranging from ~20 (but with a 10–15% 1σ uncertainty which makes this value within error of the ~18 chondritic Nb/Ta value) to significantly subchondritic (~10).

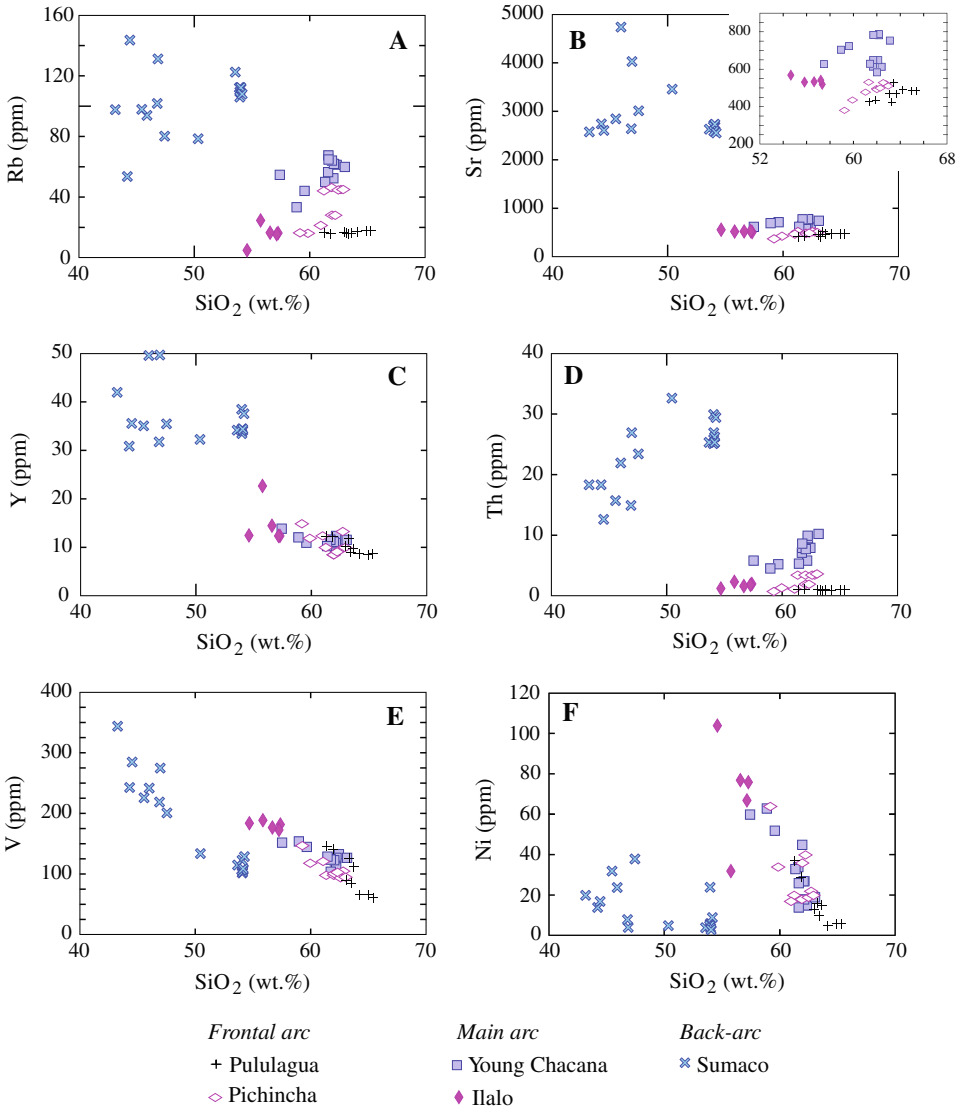

Fig. 4 Trace element variations in rocks of the studied volcanoes

Back-arc volcano (Sumaco)

Products of the back-arc Sumaco volcano plot along an alkaline trend with absarokitic to shoshonitic compositions (Fig. 3a) and, due to their alkali-rich, incompatible element-rich and SiO_2-undersaturated nature, they stand out in all major and trace element plots with respect to frontal and main arc volcanoes. Like the latter, they show decreases in Fe_2O_3, MgO, CaO, and V (as well as, not shown, TiO_2 and Sc) and similar increases of Al_2O_3, Na_2O, K_2O, Th (and U) with increasing SiO_2 (Figs. 3, 4).

Like the frontal and main arc volcanoes, Sumaco rocks are characterized by Nb and Ta negative anomalies suggesting a subduction-related origin (Fig. 5a). Sumaco rocks are strongly enriched in all incompatible elements, including the rare earths (Fig. 5a, c). REE plots are characterized by the lack of Eu negative anomalies and by strongly fractionated LREE to HREE trends ($La/Yb_N \sim 34$) with higher fractionation between MREE and HREE ($Gd/Yb_N \sim 3.0$, Fig. 5c) than at the frontal and main arc volcanoes. Like the latter, also Sumaco lavas show a good positive correlation between La/Yb and SiO_2 but not between Sr/Y and SiO_2 (Fig. 6b, c). LREE/MREE (La/Gd) and MREE/HREE (Gd/Yb) show, respectively, positive and negative correlations with SiO_2 (Fig. 6e, f), suggesting extensive clinopyroxene and amphibole fractionation, in agreement with petrographic observations.

Pb, Sr and Nd isotopes

Figure 7a, b show Pb isotope compositions of the investigated rocks in comparison with compositional fields of potential source reservoirs. Rocks of each volcanic center are characterized by small isotopic variations and plot in different fields. Sumaco products have the lowest $^{206}Pb/^{204}Pb$ values, whereas Pichincha lavas have the

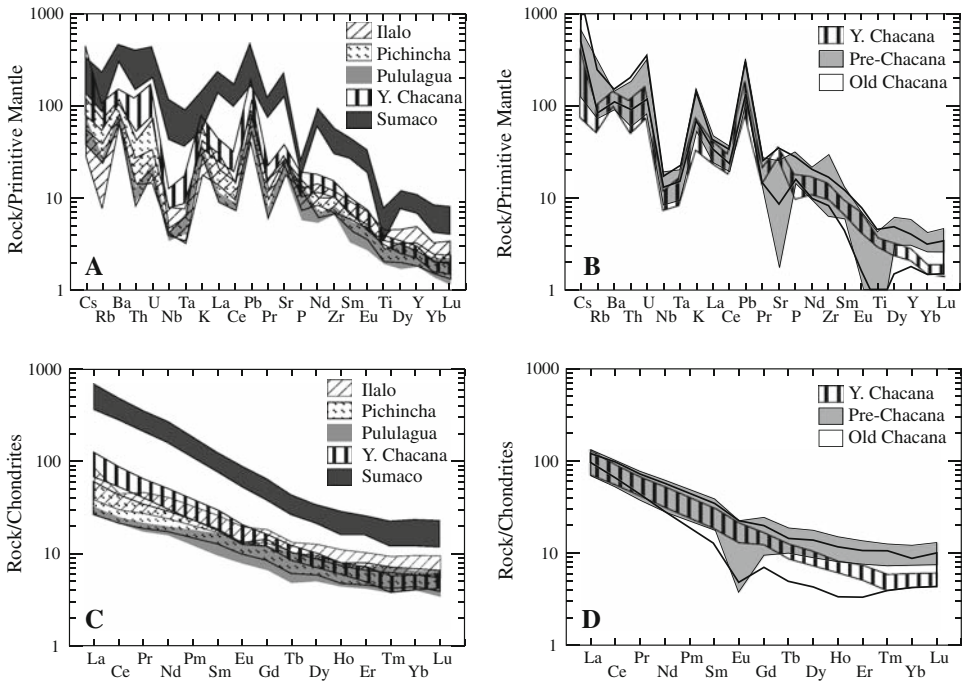

Fig. 5 **a**, **b** Primitive mantle-snormalized spidergrams of rocks of the studied volcanoes showing their subduction-related fingerprint. **c**, **d** Chondrite-normalized REE spectra of the lavas of the studied volcanoes. Normalizing values from Sun and McDonough (1989)

highest (at similar $^{207}Pb/^{204}Pb$ values between 15.55 and 15.60) with the other volcanic centers having intermediate values. All volcanic rocks investigated plot within the field of the oceanic terranes of the Western Cordillera. They plot towards slightly higher $^{208}Pb/^{204}Pb$ and $^{207}Pb/^{204}Pb$ values compared to the East Pacific Rise (EPR), Galapagos Islands (GIs) and the Galapagos Spreading Center (GSC). Chacana and, to some extent, Ilalo products are characterized by higher $^{207}Pb/^{204}Pb$ values ($\geq$15.60–15.68) than all other volcanic centers with a shift towards the compositions of the metamorphic rocks of the Eastern Cordillera.

In the Nd versus Sr isotope space (Fig. 7c), all volcanic rocks plot within the mantle array, between the Depleted MORB Mantle (DMM) and Bulk Silicate Earth (BSE) reservoirs and have positive ε_{Nd} values (except the pre-Chacana sample E05025). Young Chacana, Old Chacana and especially pre-Chacana samples have the most crustal signatures of Sr and Nd isotopes. Excluding pre-Chacana samples, all rocks overlap the $^{143}Nd/^{144}Nd$ and $^{87}Sr/^{86}Sr$ range of amphibolites and granulites of the Ecuadorian Western Cordillera and plot outside the compositional fields of the EPR and GSC. The isotopically most primitive rocks overlap the field of oceanic terranes of the Western Cordillera and Coastal Plain of Ecuador as well as that of GIs (Fig.7c).

In the Sr versus Pb isotope space (Fig. 7d), all recent volcanic rocks plot above the EPR, GIs and GSC fields and largely overlap the field of the oceanic terranes of the Western Cordillera and Costal Plain of Ecuador, that of the amphibolites and granulites of the Western Cordillera, and that of the Jurassic intrusions of the Sub-Andean Zone.

Despite the restricted range of isotopic values, rocks of all volcanic centers display more or less correlated variations of Sr, Pb, and Nd isotope ratios with major and trace elements (Fig. 8 shows some of the best correlations), suggesting the occurrence of assimilation-fractional crystallization (AFC) and/or mixing processes. Pululagua lavas are characterized by increasing $^{87}Sr/^{86}Sr$ values with evolution (Fig. 8a), whereas Pichincha lavas are characterized by decreasing $^{87}Sr/^{86}Sr$ values (Fig. 8b), suggesting assimilation of isotopically different materials below the two volcanic centers, despite the short distance separating them (Fig. 1b). Similar correlations also exist for Pb isotopes at Pichincha, indicating assimilation of/mixing with more radiogenic material (Fig. 8c). At both volcanic centers, decreasing ε_{Nd} values are accompanied by roughly increasing LREE/MREE (La/Gd) and decreasing MREE/HREE (Gd/Yb) values (Fig. 8d, e), suggesting amphibole fractionation concomitant with assimilation of the low ε_{Nd} material or mixing with low ε_{Nd} magmas from which amphibole has fractionated (see also the correlation between Nb/Ta and SiO_2, Fig. 6g).

Young Chacana samples display trends between isotopic ratios and several evolution indices, indicating assimilation of/mixing with radiogenic material in terms of both lead and strontium isotopes (Fig. 8f, g), whereas there is no correlation with Nd isotopes. It is worth noting that, whereas both Pichincha and Young Chacana rocks are characterized by assimilation of material with elevated $^{206}Pb/^{204}Pb$ composition, this material is different in the two cases. This is suggested by the fact that Young Chacana samples are also characterized by increasing

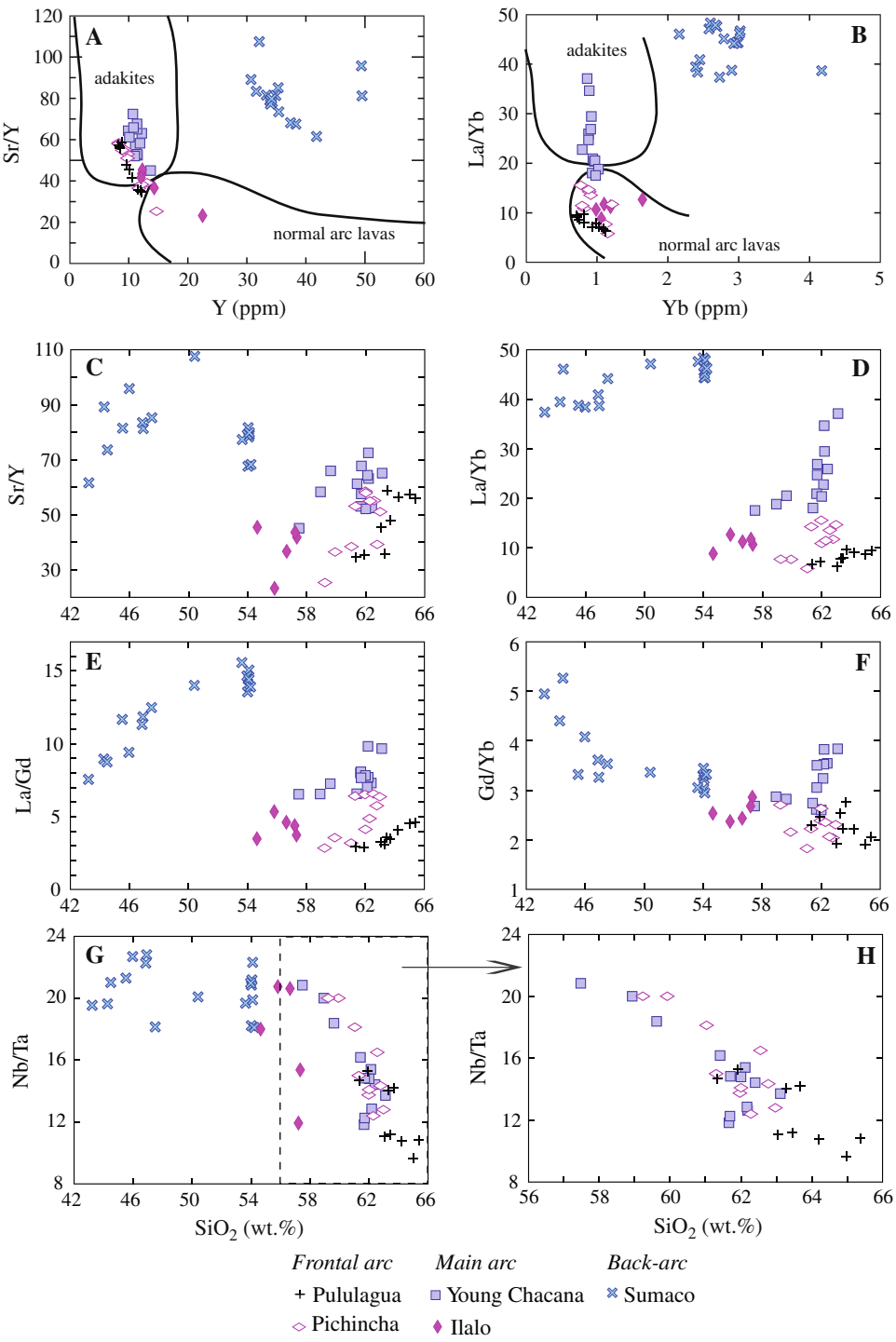

Fig. 6 Plots of Sr/Y versus Y, La/Yb versus Yb and of the variations of Sr/Y, La/Yb, La/Gd, Gd/Yb, and Nb/Ta with SiO_2 for rocks of the studied volcanoes. The adakite and "normal" arc rocks fields are from Castillo et al. (1999)

$^{207}Pb/^{204}Pb$ with evolution (not shown, but see the wide range of $^{207}Pb/^{204}Pb$ for Chacana in Fig. 7b) whereas Pichincha rocks have constant $^{207}Pb/^{204}Pb$ despite the variation in $^{206}Pb/^{204}Pb$ values (Fig. 7b).

At Sumaco only Pb isotopes display well-correlated trends with evolution indices (Fig. 8h). Sumaco volcanic rocks are the only ones that exhibit a correlation of increasing evolution with decreasing $^{206}Pb/^{204}Pb$ ratios. The lack of correlations involving Sr and Nd isotopes is expected because Sumaco magmas are extremely enriched in Sr (>2,500 ppm) and Nd (>70 ppm) and are therefore insensitive to any contamination process, besides the fact that Sr isotopic compositions of the assimilant are similar to those of the Sumaco lavas (Fig. 7c).

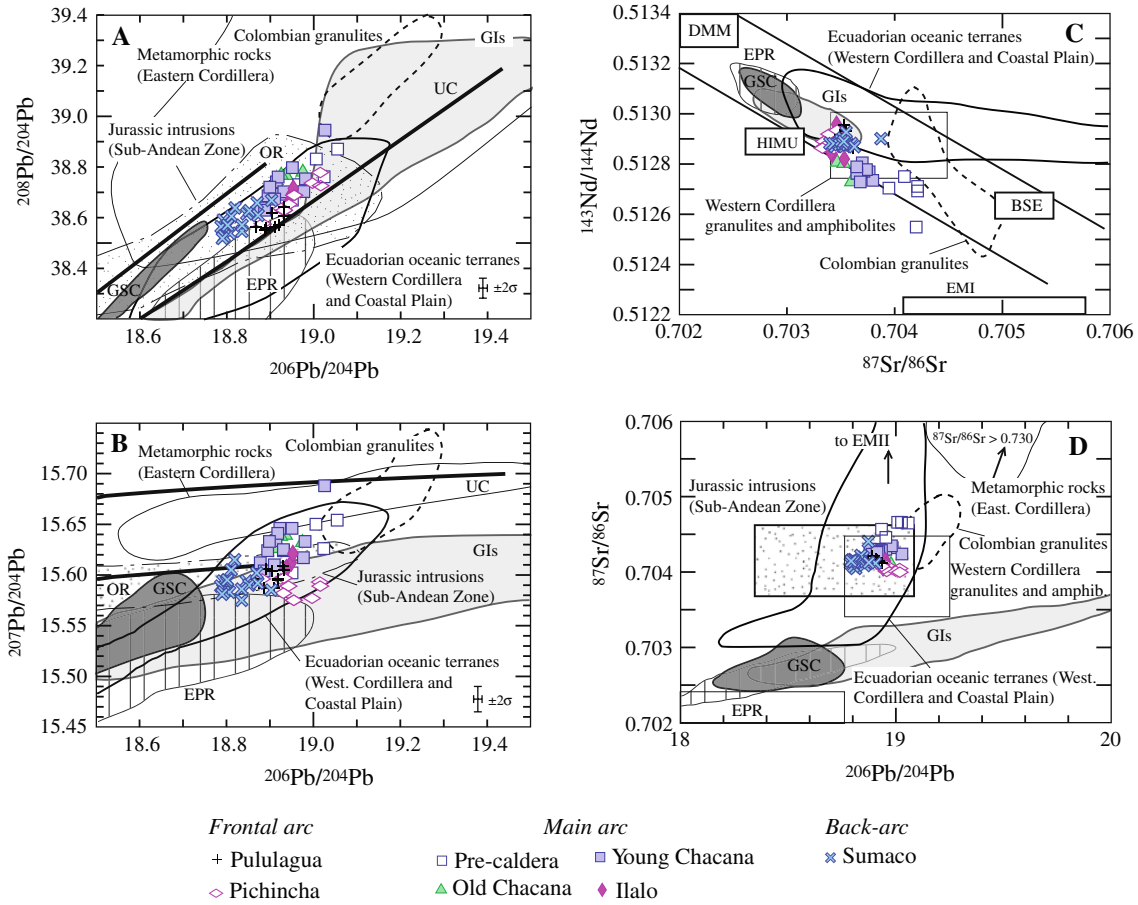

Fig. 7 Pb, Nd and Sr isotope plots of rocks of the studied volcanoes compared with fields of various potential source reservoirs and rocks (data from Zindler and Hart 1986; White et al. 1993; Litherland et al. 1994; Chiaradia and Fontboté 2001; Mamberti et al. 2003; Chiaradia et al. 2004b; Amórtegui 2007; Weber et al. 2002; Chiaradia, unpublished data). Upper crust (*UC*) and orogen (*OR*) evolution curves are from Zartman and Doe (1981). Other abbreviations: *GSC* Galapagos Spreading Center, *EPR* East Pacific Rise, *GIs* Galapagos Islands, *DMM* Depleted MORB Mantle, *HIMU* High μ, *BSE* Bulk Silicate Earth, *EMI* Enriched Mantle I. Except where reported, 2σ error bars are smaller than symbol sizes

Discussion

Across-arc geochemical variations

Primitive mantle-normalized plots of samples from all volcanic centers display features that are typical for subduction-related magmatism, such as LILE enrichment as well as Nb and Ta negative anomalies (Fig. 5). Systematic across-arc increase in incompatible elements and relative decrease in fluid-mobile elements (Fig. 9), typical for arcs worldwide (Dickinson 1975; Stolper and Newman 1994; Davidson and De Silva 1995; Ryan et al. 1995), suggest derivation of the Ecuadorian magmatic rocks from progressively smaller degrees of mantle melting towards the back-arc, induced by decreasing amounts of fluids released from the subducted slab (see also Barragan et al. 1998; Bourdon et al. 2002; Bryant et al. 2006). The low degree of partial melting in the back-arc could explain the extreme enrichment in incompatible elements of Sumaco lavas (see also Barragan et al. 1998).

A major point of discussion in the genesis of subduction-related magmas is the nature of the fluids metasomatizing the mantle wedge, whether aqueous fluids or melts (e.g., Class et al. 2000), although Kessel et al. (2005) have shown that the difference between melt-induced and aqueous fluid-induced metasomatism in subduction zones is no longer valid at $P > 5$ GPa (supercritical fluid). The consistent decrease of the ratios of aqueous fluid-mobile to aqueous fluid-immobile elements (Ba/Nb, Ba/La, Pb/Ce, U/Nb) from the front (Pululagua, Pichincha) to the back-arc (Sumaco) (Fig. 9) is consistent with an aqueous fluid being released from the slab although this probably does not dismiss the concomitant release of a melt. Th/La values (Fig. 9f), a potential proxy for sediment melt contribution, are essentially constant across the arc, the higher values of some Chacana samples being related to crustal assimilation (Th is correlated with $^{207}Pb/^{204}Pb$ at Chacana: not shown). The Nb/Ta ratio shows an overall increase of minimum values towards the back-arc but,

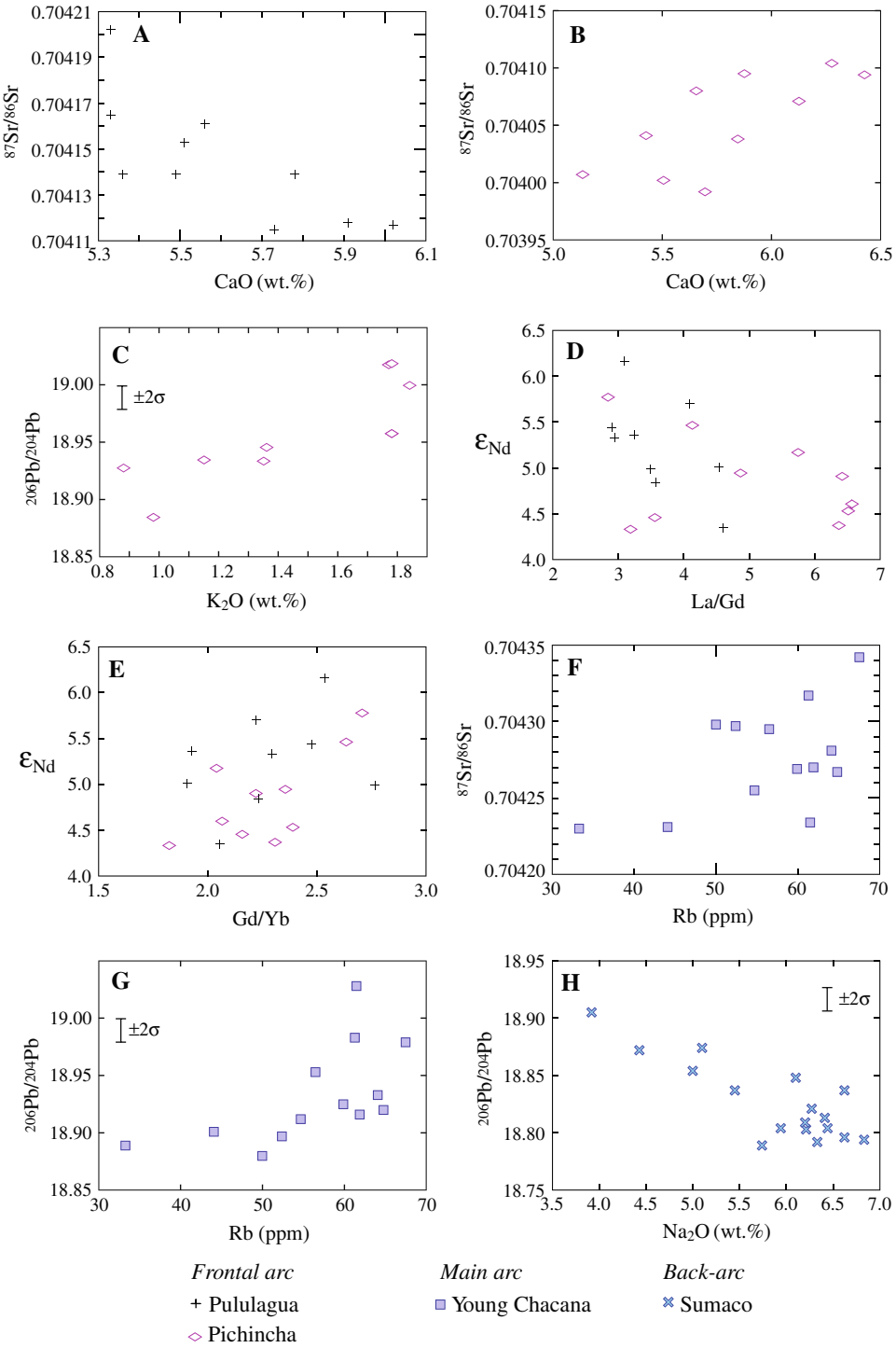

Fig. 8 Correlations between radiogenic isotopes and evolution indices at the investigated volcanic centers. Except where reported, the 2σ error bars are smaller than symbol sizes

except Pululagua, has virtually constant maximum values (~20, Fig. 9d). Variations within volcanic centers of the frontal and main arc (except Ilalo), but not of the back-arc, are negatively correlated with SiO_2 (Fig. 6g, h) suggesting that the magmatic evolution is controlled by amphibole fractionation at depth, which lowers the Nb/Ta ratio of derivative liquids (see also Tiepolo et al. 2000; Alonso-Perez 2006), or alternatively by assimilation of low Nb/Ta crustal rocks and/or their partial melts (e.g., Garrido and Bodinier 2005; see also below). The La/Yb ratio gradually increases towards the back-arc (see also Vanek et al. 1994; Bryant et al. 2006), which could indicate an increasing amount of residual garnet in the mantle source of the magmas of the main and back-arc. However, variable increases of La/Yb with SiO_2 (Fig. 6) at each volcanic center indicate that fractionation and assimilation effects

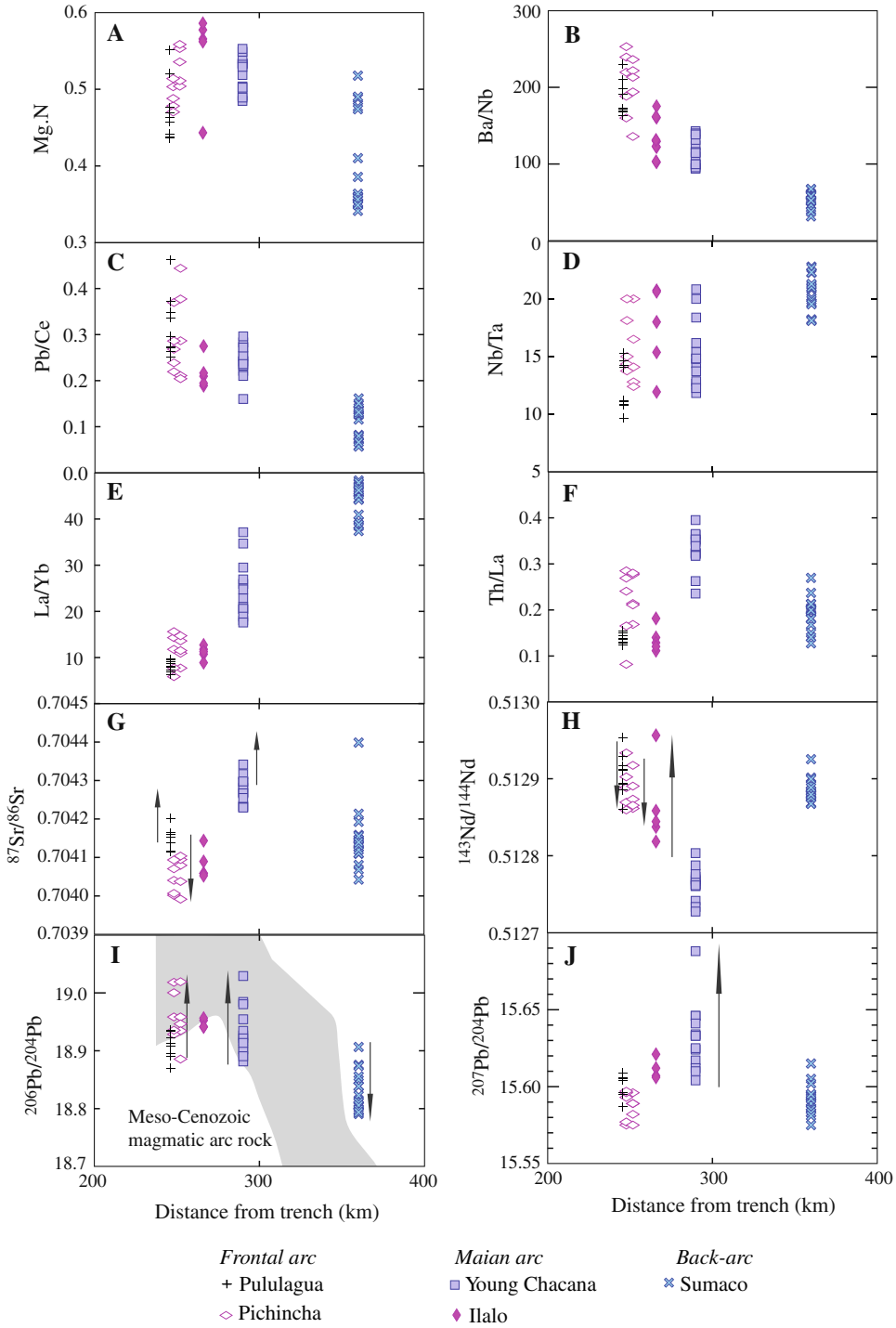

Fig. 9 Across-arc variations of trace element ratios and radiogenic isotopes of rocks of the investigated volcanoes. *Arrows* indicate evolutionary trends determined on the basis of correlations between radiogenic isotopes and major/trace elements as in Fig. 8 (the tip of the *arrow* points to the direction of the assimilated material). The *shaded field* in Fig. 9i represents isotopic compositions of Meso-Cenozoic magmatic arc rocks of Ecuador (data from Chiaradia et al. 2004b)

(besides source effects) are also responsible for across-arc variations of LREE/HREE (see below).

Radiogenic isotopes display systematic across-arc changes (Fig. 9g–j). Sr and Nd isotopes (Fig. 9g–h) have primitive values in the frontal arc (Pululagua and Pichincha), then gradually shift through Ilalo to more evolved values in the main arc (Chacana) and go back to more primitive values in the back-arc (Sumaco). This trend has been considered (Barragan et al. 1998; Bourdon et al. 2003) as the result of a slight crustal contamination in coincidence with the main arc of an otherwise isotopically homogeneous mantle across the arc. We agree with this latter interpretation, as the least crust-contaminated rocks (base of the arrows in Fig. 9g) have virtually the same Sr isotope composition across the arc. However, we point out that crustal contamination does occur also at the frontal and

back-arc volcanoes, as shown by the correlated trends between radiogenic isotopes and major/trace elements (Fig. 8) and by petrographic observations. The apparent higher contamination in coincidence with the main arc is due to different isotopic compositions of the assimilant in the frontal, main and back-arc. Further evidence for the involvement of crustal rocks in the genesis of the Ecuadorian lavas throughout the arc is given by the overall decreasing $^{206}Pb/^{204}Pb$ values of the volcanic rocks from the front to the back-arc, similar to an equivalent $^{206}Pb/^{204}Pb$ trend of the Cenozoic and Mesozoic arc rocks on which the Quaternary volcanic centers are built (Fig. 9i). The least crust-contaminated rocks (base of the arrows in Fig. 9g–j) have similar $^{206}Pb/^{204}Pb$ ratio across the arc, which likely reflects the homogeneous mantle wedge composition under Ecuador (see above). $^{207}Pb/^{204}Pb$ values show a gradual increase from the frontal to the main arc and then decrease again in the back-arc (Fig. 9j), similar to Sr isotopic compositions, suggesting contamination by ^{207}Pb-rich lithologies in the main arc.

Origin of adakite-like signatures of the frontal and main arc volcanic centers

The adakite-like signatures of the frontal and main arc volcanoes of Ecuador have been interpreted in two ways. One hypothesis is that the signature is retained from slab melting (e.g., Bourdon et al. 2002, 2003; Samaniego et al. 2002; Hidalgo et al. 2007). Another hypothesis considers them as resulting from lower crustal assimilation-fractional crystallization (AFC) and partial melting processes (e.g., Kilian et al. 1995; Monzier et al. 1999; Garrison and Davidson 2003; Chiaradia et al. 2004a; Garrison et al. 2006).

Major and trace element variations as well as radiogenic isotope compositions coupled to petrographic observations indicate that the adakite-like products of each volcanic center investigated are the result of multiple magmatic processes, including fractional crystallization, assimilation and mixing within the crust. Resolving the relative contributions from each one of the above processes is almost impossible especially when trying to distinguish between assimilation accompanied by fractional crystallization (AFC) and simple mixing (magma–solid, magma–magma) processes.

Surprisingly, little attention has been given by past studies to petrographic investigations, despite the fact that there is widespread evidence for open-system processes at all volcanic centers of Ecuador. The occurrence of centimeter- to micrometer-sized mafic granulite xenoliths, of pyroxene clots and amphibole-/pyroxene-bearing cumulates in lavas of the investigated frontal and main arc volcanic centers indicate that primitive melts have incorporated, disaggregated, partially melted and eventually digested mafic to intermediate rocks as well as cumulates, at depth but probably also during magma ascent (see also Annen et al. 2006; Blundy et al. 2006). Additionally, resorption, partial or complete melting of different xenocrysts such as plagioclase, amphibole, pyroxene, and quartz as well as inverse geochemical zoning in plagioclase and pyroxene (see above) indicate that mixing between magmas of contrasting compositions has played an important role in the petrogenesis of frontal and main arc magmas (see also Garrison et al. 2006). Although we do not rule out the possibility of producing Si-rich melts during subduction (see also van Keken et al. 2002; Kincaid and Griffiths 2004; Kessel et al. 2005; Grove et al. 2006), it is unlikely that in the case of Ecuador slab melts or melts derived from a mantle metasomatized by slab melts would have survived up to the surface with pristine signatures given the evidence for the above interaction processes within the crust.

Adakitic indices (e.g., Sr/Y, La/Yb, Na_2O, Sr, Al_2O_3) and Nb/Ta values correlate with fractionation indices (e.g., SiO_2, Ni) within each volcanic center of the frontal and main arc (Figs. 3, 4, 6). Such correlations can be explained by a process in which mantle-derived hydrous basaltic melts fractionate at depth a liquidus assemblage initially dominated by clinopyroxene, amphibole ± garnet (Green 1972, 1982; Müntener and Ulmer 2006; Alonso-Perez et al. 2009). This results in the incompatible behavior of Sr, Na_2O, LREE and to some extent Al_2O_3 and in the compatible behavior of Y and HREE. Scatter in the correlation trends is eventually produced by the concurrence of different igneous processes such as AFC and mixing as well as by subsequent fractionation and mixing at shallower crustal levels. Also under this point of view adakite-like signatures seem to be linked to magmatic evolution rather than to source processes (i.e., slab melting and slab melt–mantle interaction). We emphasize that lavas with the strongest adakite-like features within each frontal and main arc volcanic complex have Ni contents (Ni = 10 at Pululagua; Ni = 18 at Pichincha and Chacana) below those of adakites generated by slab melting (Ni = 20 ppm, Martin et al. 2005) and far below those of slab melts that are presumed to have interacted with a peridotitic mantle (Ni = 103 ppm, Martin et al. 2005), and that the Ni contents show a rough inverse correlation with adakitic indices (Sr/Y, La/Yb).

The correlations between fractionation (including adakitic) indices and radiogenic isotopes at the frontal and main arc volcanic centers (Fig. 8) are difficult to reconcile with the slab melt hypothesis and are best explained by either (1) initial fractionation of mantle-derived basaltic melts outside the stability field of plagioclase and within that of clinopyroxene, amphibole ± garnet accompanied by concomitant assimilation of crustal material, (2) mixing of the mantle-derived melts with crustal melts formed in

the clinopyroxene, amphibole ± garnet stability field, or (3) mixing of mantle-derived melts with their precursors that have already assimilated crustal rocks and fractionated at depth [process (1) above] or have already mixed with crustal melts [process (2) above]. The small absolute isotopic shifts for the concomitant major/trace element variations at all volcanic centers (Fig. 8) suggest assimilation of/mixing with materials that are isotopically similar to the mantle-derived magmas. Pichincha lavas host mafic granulite xenoliths (sample E05130a) with Nd ($^{143}Nd/^{144}Nd = 0.512882$) and Sr ($^{87}Sr/^{86}Sr = 0.70390$) isotopic compositions slightly less radiogenic than the host lava (0.512934 and 0.704094, respectively), and compatible with the non-radiogenic end-member of the observed AFC/mixing trends (Fig. 8d, e). The isotopic composition of this mafic granulite xenolith falls within the compositional range of lower crustal granulites and amphibolites of the Western Cordillera of Ecuador (Fig. 7). Altogether these rocks have a range of Sr, Pb and Nd isotopic compositions similar to those of the frontal arc lavas, and, at the same time, compatible with being the assimilant for products of the frontal arc volcanoes (plus Ilalo?). The granulites and amphibolites of the Western Cordillera of Ecuador have geochemical signatures suggesting that they are the lower crust metamorphic equivalents of the accreted oceanic plateau rocks of the Western Cordillera (Amórtegui et al. 2005; Amórtegui 2007), but have $^{143}Nd/^{144}Nd$ values shifted towards the present-day volcanism compared to their non-metamorphosed equivalents (Ecuadorian oceanic terranes in Fig. 7a). In a long-lived magmatic arc system, the mid to lower crust section will be continuously refined chemically and isotopically towards the compositions of the uprising melts through MASH (Melting–Storage–Assimilation–Homogenization)-type processes (Hildreth and Moorbath 1988; see also Dungan et al. 2001; Lee et al. 2006). Therefore, the isotopic compositions of the exposed basement rocks (often used in modeling calculations) are not necessarily the same as those of the rocks assimilated at deeper crustal levels in magmatic arcs where they have gone through the magmatic refining process.

The assimilant at Chacana is different as indicated by the overall more radiogenic $^{207}Pb/^{204}Pb$ and $^{87}Sr/^{86}Sr$ and less radiogenic Nd isotopic signatures and is consistent with the Chacana volcanic center being situated above Jurassic Alao island arc metabasalts as well as Paleozoic schists and gneisses of the continental Loja terrane (Fig. 1b) characterized by elevated $^{207}Pb/^{204}Pb$ and $^{87}Sr/^{86}Sr$ values (Fig. 7b). Also these rocks could have been modified at depth by magmatic refining processes associated with the Jurassic Alao arc and/or the Quaternary arc.

Thus, a petrogenetic model for the adakite-like signatures of the frontal and main arc Ecuadorian magmas must be able to explain: (1) assimilation of mafic granulite rocks as well as amphibole- and/or clinopyroxene-bearing cumulates; (2) magma mixing processes; (3) increasing adakitic indices with evolution of the magmas; (4) correlations between evolution indices (including adakitic indices) and radiogenic isotopes for limited absolute variations of the latter. A MASH-type model (Hildreth and Moorbath 1988) with its recent numerical formulations and variations (e.g., Petford and Gallagher 2001; Dufek and Bergantz 2005, the deep hot zone magma generation model of Annen et al. 2006) explains most of these features.

Applying this model to the Ecuadorian frontal and main arc magma genesis, a hot zone forms at lower- to mid-crustal levels by the intrusions of mantle-derived basaltic melts which start to crystallize within the stability field of clinopyroxene, amphibole ± garnet (e.g., Green 1972; Green 1982; Müntener et al. 2001; Müntener and Ulmer 2006; Alonso-Perez et al. 2009). Even if mantle-derived melts are not H_2O-rich to promote an early crystallization of amphibole (± garnet), sustained crystallization of anhydrous phases (e.g., pyroxene and olivine) at high pressures will drive liquids towards H_2O-rich compositions. On the other hand, melts may be formed by partial melting of a mafic lower- to mid-crust, refined by variably older magmatic arc episodes. Formation and subsequent mixing of the mantle-derived residual melts and crust-derived partial melts will occur after an incubation time depending on the geotherm, magma emplacement rate and depth (Annen et al. 2006). Continuously inflowing mantle-derived basaltic melts will mix with hybrid melts formed by the above process and may thus produce the variably correlated trends of isotope and major/trace elements observed for the Ecuadorian volcanoes. Because of the lower crustal geochemical refinement inherent to such a process and the continuous homogenization between crustal and mantle-derived melts, the chemical and isotopic variability of the magmas is expected to become smaller with time (consistent with small compositional ranges at each volcanic center of the frontal and main arc). Similar petrogenetic processes are likely to occur elsewhere in continental arcs (see also Dungan et al. 2001; Dungan and Davidson 2004; Lee et al. 2006; Davidson et al. 2007) and have already been proposed for individual Colombian and Ecuadorian volcanoes (Galeras, Sangay, Cotopaxi, Calvache and Williams 1997; Monzier et al. 1999; Garrison et al. 2006, respectively). Further mixing and fractionation is likely to occur at shallower crustal levels and/or during magma ascent promoting additional differentiation and scatter in the observed trends.

Partial melting, incorporation, and disaggregation of lower- to mid-crustal mafic rocks into mantle-derived magmas require a high thermal flux and/or a long-lived magmatic system (e.g., Annen et al. 2006; Dufek and

Bergantz 2005). Amórtegui et al. (2005) have proposed a high thermal flux underneath the Western Cordillera since the Miocene. Incubation times leading to a maximum melt productivity from lower crust partial melting at 30 km depth and with an average basaltic melt intrusion rate of 5 mm/year must be >1 My (Annen et al. 2006). Such incubation times are consistent with the long-lived magmatic history of several volcanic centers of both the frontal (Rucu Pichincha is at least 0.85 My old, Fornari et al. 2004) and main arc (Chacana is more than 0.85 My old, Ilalo is 1.6 My old; see above).

Modeling igneous processes at the frontal and main arc volcanic centers

Although the correlations between radiogenic isotopes and most major and trace elements may lend themselves to chemical modeling for the frontal and main arc volcanoes, we have seen that the petrogenesis of the frontal and main arc Ecuadorian lavas is the result of multiple processes that make quantitative modeling using simple mixing or AFC equations not very meaningful. This is reflected by the inconsistent estimates of fractionation and assimilation that we have obtained at single volcanic centers using various mixing and AFC models. Additionally, the isotopic compositions and element concentrations of a refined lower crust assimilant are largely unconstrained and little isotopic and trace element changes result in widely different assimilation estimates.

Given these uncertainties, we prefer to illustrate and discuss a simple REE modeling to gain some information on the role of garnet fractionation in the petrogenesis of Ecuadorian lavas. Figure 10 shows the results of AFC modeling and mixing processes in the La/Yb versus Yb space. For both process, we have modeled trends of an oceanic island arc basaltic parent (IAB in Table 1; Fig. 10) fractionating and assimilating/mixing with two arbitrarily chosen crustal rocks/melts of a deep hot zone: (1) a lithology/melt with La and Yb contents similar to those of the most evolved rock of each center (A′ for Pululalgua, B′ for Pichincha, C′ for Young Chacana, Table 1), simulating an immature deep hot zone (which is characterized by more evolved geochemical signatures, see Annen et al. 2006), and (2) a lithology/melt with La and Yb contents similar to those of the least evolved rock of each center (AB for Pululagua and Pichincha and C for Young Chacana, Table 1), simulating a mature deep hot zone.

It is important to note that in the AFC process the position and shape of the modeled trends in the La/Yb versus Yb space is much more sensitive to D_{Yb} and D_{La} values than to the R value (mass of the assimilant/mass of the crystallized magma), which instead has a stronger control on the amount of material assimilated (being directly linked to F = mass of magma remaining/mass of initial magma). Therefore, our modeling provides semi-quantitative information on bulk fractionation coefficients of La and Yb, but not on assimilation estimates. The same reasoning applies to mixing processes in which the mixing end-members were arbitrarily chosen as described above because they were not identifiable in the investigated volcanic suites.

Despite the uncertainties discussed above, there are some consistent outcomes from our modeling (Fig. 10):

1. AFC and mixing modeling closely reproduces the trends at Pichincha and Pululagua independently of the choice of the different end-members discussed above and summarized in Table 1. Mixing and AFC processes fail to reproduce the Chacana trend when an IAB parent is used. However, the Chacana trend can be reproduced by a 2-step process, e.g., initial AFC of the IAB parent (to $F = 0.1$, Fig. 10a) followed by mixing with the C′ end-member (Fig. 10c).
2. For the mixing process, the low (<1 ppm) Yb contents of the more evolved (i.e., SiO_2-richer, higher in La/Yb and lower in Yb) end-members (A′, B′, C′, Table 1) at all volcanic centers probably require garnet fractionation (either as magmatic crystallization, although garnet was not found in the investigated lavas, or as a restitic phase) in the source of these end-members.
3. In the AFC process, bulk D_{Yb} is >1 at all volcanic centers (Table 1). This implies fractionation between <1% and up to a maximum of 2.5% of garnet, assuming a D_{Yb} of 50 between garnet and andesitic melt (Irving and Frey 1976), a fractionating assemblage consisting, besides garnet, of amphibole and clinopyroxene in a ratio of 4:3, and D_{Yb} of 1.5 for amphibole–andesite and of 0.9 for clinopyroxene–andesite (D_{Yb} values from GERM, http://earthref.org/GERM/). Changing the proportions of the fractionating assemblage will result in slightly higher or lower estimates of garnet fractionation. The latter may occur either in the form of magmatic garnet crystallization or as a restitic phase in the assimilant.
4. In AFC models, bulk D_{La} is >0 in the frontal arc volcanoes (Table 1), suggesting either fractionation of a mineral phase(s) that extracts LREE from the magma or a significant contribution of the oceanic plateau crust (which forms the basement of the Western Cordillera of Ecuador and is characterized by flat REE spectra) to the genesis of the frontal arc magmas.

Back-arc (Sumaco)

Absarokite rocks like those of Sumaco generally result from a low degree (1–5%) of partial melting of a highly

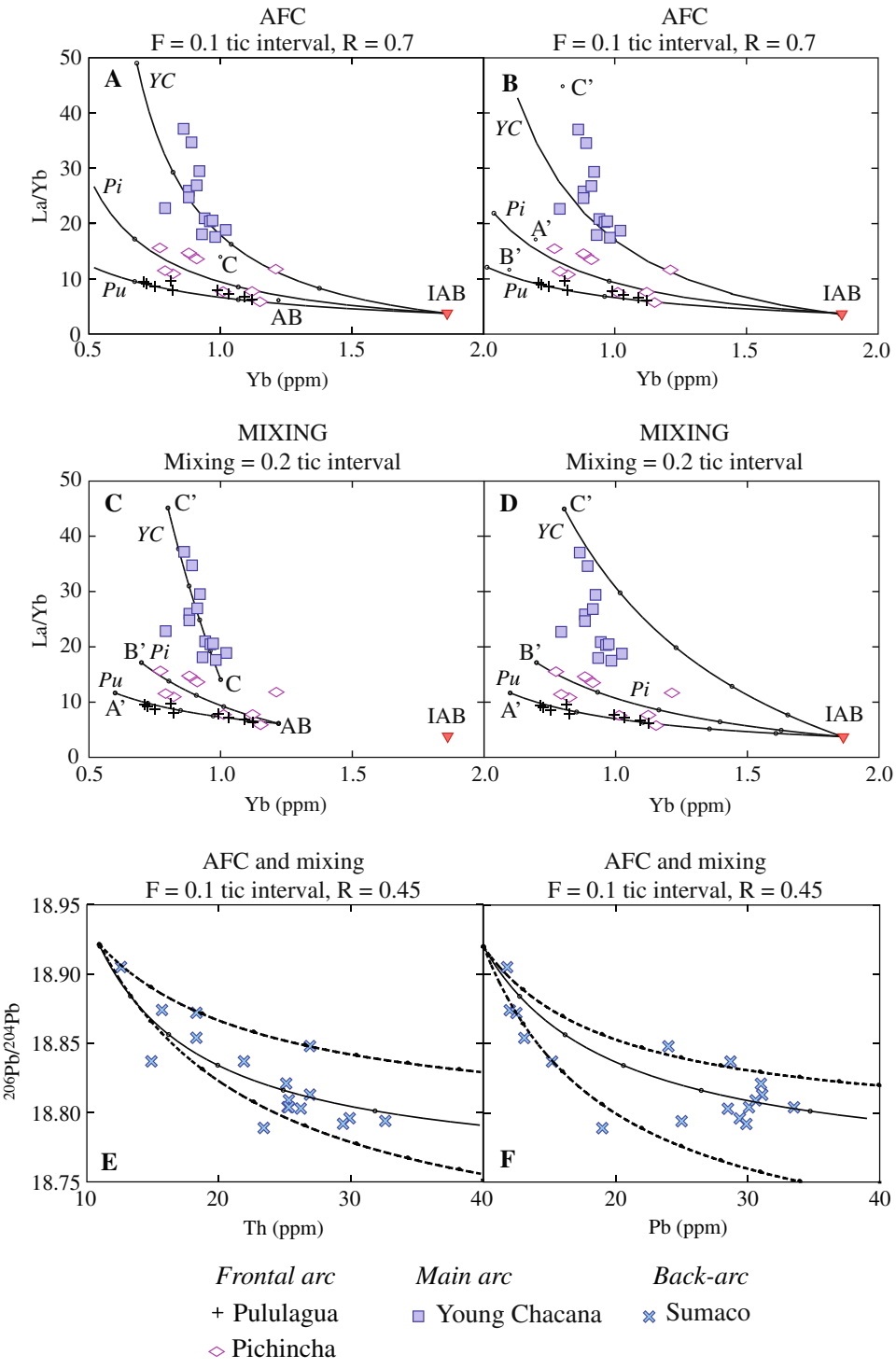

Fig. 10 AFC (*panels* **a**, **b**) and mixing (*panels* **c**, **d**) modeling of the correlations between La/Yb and Yb at Pululagua, Pichincha, and Young Chacana, using the equations of DePaolo (1981) and simple two-end-member mixing equations. The end-members used in the modeling and their element concentrations are reported in Table 1 and discussed in the text. Modeled curves are shown only for the bulk partition coefficients of La and Yb reported in Table 1, which satisfy the best fit to the rock data. AFC (*solid line*) and mixing (*dashed lines*) modeling of the correlations of $^{206}Pb/^{204}Pb$ with Th and Pb at Sumaco (*panels* **e**, **f**) using the equations of DePaolo (1981) and simple mixing equations. End-member compositions are reported in Table 2. The two modeled mixing lines suggest that scatter can be explained by slight variations in the isotopic composition of the assimilant. *F* melt mass remaining (Mr)/initial melt mass (Mi); *R* mass of assimilated material (Ma)/mass of crystallized melt (Mc). *IAB* average oceanic island arc basalt from Kelemen et al. (2004)

metasomatized mantle (e.g., Tatsumi and Koyaguchi 1989; Edwards et al. 1994), probably containing phlogopite (see also Bourdon et al. 2003; Hoffer et al. 2008). As we have already pointed out, the Nb and Ta negative anomalies of absarokitic and shoshonitic rocks of the back-arc Sumaco volcano suggest that such metasomatism was related to a subduction zone (see also Barragan et al. 1998; Bourdon et al. 2003). Quaternary subduction could have been responsible for such metasomatism (e.g., Bourdon et al. 2003), but it cannot be excluded that metasomatism occurred also during the Late Jurassic, when a continental arc was established on the western edge of the Amazon craton (e.g., Litherland et al. 1994; Chiaradia et al., 2009) after which subduction-related magmatism ceased until the

Table 1 End-members used for modeling AFC trends at the Pululagua, Pichincha, and Young Chacana volcanic centers (Fig. 10a, b)

Volcanic center	Parent	Assimilant	D_{Yb}	D_{La}
Pululagua AFC (Fig. 10a)	IAB[a]	AB	2.5	1.2
	La 7.01 ppm	La 7.5 ppm		
	Yb 1.86 ppm	Yb 1.22 ppm		
Pululagua AFC (Fig. 10b)	IAB	B′	2.5	1.2
	La 7.01 ppm	La 12 ppm		
	Yb 1.86 ppm	Yb 0.7 ppm		
Pichincha AFC (Fig. 10a)	IAB	AB	2.5	0.2
	La 7.01 ppm	La 7.5 ppm		
	Yb 1.86 ppm	Yb 1.22 ppm		
Pichincha AFC (Fig. 10b)	IAB	A′	2.5	0.5
	La 7.01 ppm	La 7 ppm		
	Yb 1.86 ppm	Yb 0.6 ppm		
Young Chacana AFC (Fig. 10a)	IAB	C	1.6	0
	La 7.01 ppm	La 14 ppm		
	Yb 1.86 ppm	Yb 1 ppm		
Young Chacana AFC (Fig. 10b)	IAB	C′	2.5	0
	La 7.01 ppm	La 36 ppm		
	Yb 1.86 ppm	Yb 0.8 ppm		

The same end-members are also used for mixing trends (Figs. 10c, d)

[a] Data of average oceanic Island Arc basalt (IAB) from Kelemen et al. (2004). Data for the other end-members chosen as explained in the text

Quaternary. The high incompatible element concentrations and La/Yb values of Sumaco lavas could result from a small degree of partial melting of a metasomatized garnet–phlogopite-bearing lherzolite (see also Hoffer et al. 2008) or, alternatively, by a higher degree of melting of hornblende-rich mantle veins (Pilet et al. 2008).

Evolutionary trends of Sumaco lavas in major and trace element plots indicate fractionation of Fe-, Mg-bearing silicates (olivine, clinopyroxene, and amphibole are phenocrysts in Sumaco lavas) but not of plagioclase in agreement with petrographic observations showing that plagioclase phenocrysts appear only in the most evolved rocks of the Sumaco volcano. However, Sumaco lavas also show assimilation of non-radiogenic Pb material as indicated by the correlations between various major/trace elements and $^{206}Pb/^{204}Pb$ values (e.g., Fig. 8h). The non-radiogenic Pb assimilated in this case is consistent with isotopic compositions of the Jurassic intrusions of the Sub-Andean zone (Fig. 7), upon which Sumaco volcano sits.

Modeling igneous processes at Sumaco volcano

Both mixing and AFC models are able to reproduce closely the observed correlations between Pb isotopes and evolution indices (e.g., Th and Pb in Fig. 10). Importantly, in the case of AFC, model estimates of assimilation and fractional crystallization are consistent for the two trends, which was not the case for the frontal and main arc volcanoes (see above). This probably suggests an evolution of Sumaco magmas through simpler processes than at the frontal and main arc. Nonetheless, absolute values of assimilation remain unconstrained due to uncertainties in the isotopic and element composition of the assimilant.

For the assimilant we have used Th and Pb concentrations of a diorite sample (E99022, Chiaradia et al. 2004b) of the Jurassic Zamora batholith (Table 2) and Pb isotope compositions of Jurassic intrusive rocks of the western edge of the Amazon craton (on which Sumaco sits). The latter display a large range of variability between 18.36 and 19.26, with a median value in the range 18.6–18.8. For AFC modeling, we have chosen an arbitrary $^{206}Pb/^{204}Pb$ value of 18.64 for the assimilant (Table 2), which closely reproduces the observed trends for $R = 0.45$. In this case, F is 50% and the assimilation is about 30% (Fig. 10e, f), which is a reasonable estimate for mafic rocks assimilating fertile material close to its solidus temperature (e.g., Matile et al. 2000). Changing the $^{206}Pb/^{204}Pb$ to higher or lower values requires significant changes of Th and Pb of the

Table 2 Element concentrations and Pb isotope compositions of the end-members used for modeling AFC and mixing trends at the Sumaco volcanic center (D_{Pb} and $D_{Th} = 0$)

End-member	Th (ppm)	Pb (ppm)	$^{206}Pb/^{204}Pb$
Parent/mix 1 (AFC and mixing models)	11	10	18.92
Assimilant (AFC model)	12	18	18.64
Mix 2 (mixing model)	50	40	18.74
Mix 3 (mixing model)	50	40	18.82

assimilant as well as significant changes in the R and F values to reproduce the observed trends. Due to the variable composition of the plutonic rocks of the western edge of the Amazon craton such changes in the trace element compositions of the assimilant are not unrealistic and rather large uncertainties on the amount of assimilation will prevail ($\sim$10–40%).

Mixing models reproduce the observed trends only if significantly high concentrations of Th and Pb (>35 ppm) are assumed for the assimilant (Table 2). Partial melting of mafic lithologies may produce melts with extremely high incompatible element concentrations (e.g., Storkey et al. 2005) and could represent the enriched end-member of the mixing. However, an AFC process is preferable in view of scant petrographic evidence for mixing processes in Sumaco lavas. The scatter around the trends might indicate assimilation of rocks with variable isotopic compositions (Fig. 10).

Transition from non-adakitic to adakite-like rocks in Ecuador

Chiaradia et al. (2004a, b) pointed out a clear difference between the geochemical evolution of Middle to Late Miocene (pre-6 Ma) non-adakitic rocks of southern Ecuador and Latest Miocene to Pliocene (post-6 Ma) adakite-like volcanic rocks. The present study (as Bourdon et al. 2002; Samaniego et al. 2002) illustrates that such an evolution is also recorded by Quaternary volcanic centers of northern Ecuador, like Chacana, with the difference that the transition from non-adakitic to adakite-like rocks in this case occurs <1 My ago.

Figure 11 shows Sr versus Pb and Pb versus Pb isotope plots for the adakite-like volcanic rocks of the Quaternary volcanic centers, for the ≥0.85 My old non-adakitic rocks of Pre-Chacana and for pre-6 Ma non-adakitic rocks of Ecuador (Chiaradia et al. 2004a). Adakite-like volcanic centers are characterized by consistently low and homogeneous $^{87}Sr/^{86}Sr$ values (0.7040–0.7044) compared to the non-adakitic rocks, which extend to $^{87}Sr/^{86}Sr$ values up to 0.706 (Fig. 11a). This reflects the different depth of evolution of adakite-like and non-adakitic rocks of Ecuador. The former evolved outside the plagioclase stability field (no negative Eu anomalies in these rocks), at lower- to mid-crustal levels, assimilating non-radiogenic mafic granulites and amphibolites. Non-adakitic rocks evolved in the stability field of plagioclase (strongly developed negative Eu anomalies in these rocks) at upper crustal levels, assimilating radiogenic Sr-bearing rocks.

Another interesting feature shown by the plots of Fig. 11 is that all adakite-like and non-adakitic rock groups define crustal assimilation trends, in which least evolved rocks (base of the arrows in Fig. 11) originate from the same area

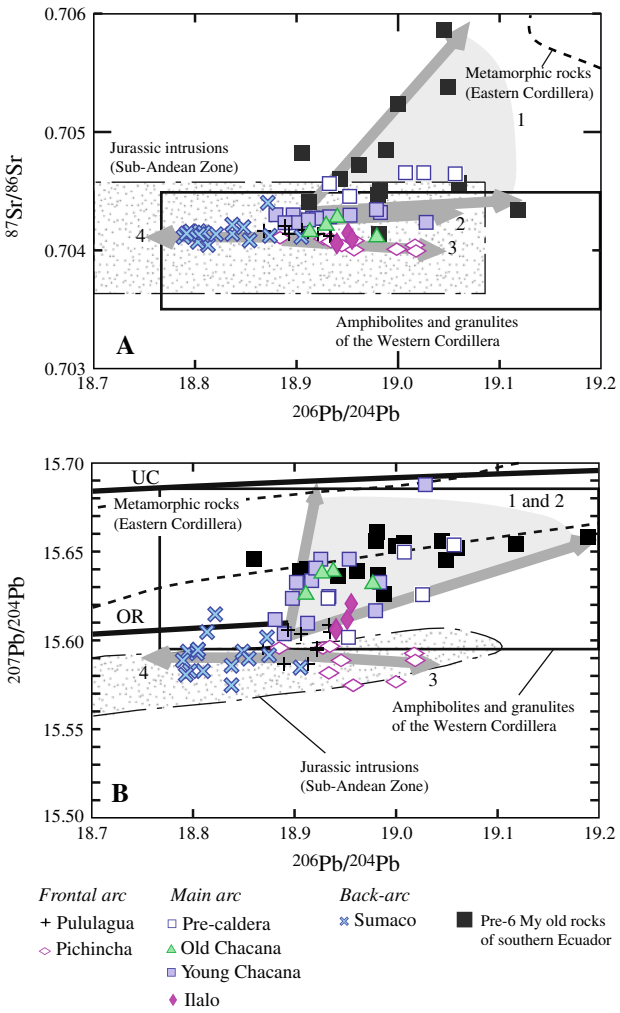

Fig. 11 Quaternary adakite-like rocks of the investigated volcanic centers, ≥0.85-My-old non-adakitic rocks of Pre-Chacana and pre-6-My-old non-adakitic rocks define roughly linear trends in the Sr–Pb (**a**) and Pb–Pb (**b**) spaces, highlighted by the *arrows*. Least evolved rocks of each one of the above rock groups, corresponding to the *base of the arrows*, plot in the same area, suggesting a common isotopic source. Evolutionary trends radiating from this common isotopic compositional area towards different points of the Sr–Pb and Pb–Pb isotopic spaces reflect assimilation of isotopically different basement rocks. Arrow legend: *1* assimilation trend for non-adakitic pre-Chacana and pre-6-My-old rocks (the fan-like, rather than linear trend towards radiogenic values, reflects assimilation of basement rocks with variable isotopic signatures); *2* assimilation trend for Young Chacana rocks; *3* assimilation trend for Pichincha rocks; *4* assimilation trend for Sumaco rocks. The spread of Pululagua rocks is too small to be highlighted at the scale of this plot. Data are from this study and Chiaradia et al. (2004b). The field of the amphibolites and granulites of the Western Cordillera are from Amórtegui (2007). Upper crust (UC) and orogen (OR) evolution curves are from Zartman and Doe (1981)

in the bidimensional isotopic spaces. This suggests that the source of both adakite-like and non-adakitic magmatism is the same (see also Chiaradia et al. 2004a), i.e., the mantle wedge enriched by a fluid component (regardless if

aqueous, supercritical or melts). Each group of rocks shows different assimilation trends, due to the heterogeneous nature of the Ecuadorian crust upon which the various volcanic centers sit and the crustal depth at which magmas evolved (see above).

A similar evolution of magmas through time from non-adakitic to adakite-like has also been observed in Tertiary lavas of the Central Andes and has been attributed to crustal thickening (e.g., Kay et al. 1991). In Ecuador, due to the rapid geochemical switch from non-adakitic to adakite-like features in less than 1 My, the subduction of the Carnegie Ridge is a more likely responsible for the increased depth of magma fractionation and consequent generation of adakite-like signatures in Quaternary magmas (Fig. 12), although concomitant crustal thickening is likely to have occurred. The collision of the Carnegie Ridge with the subduction zone has led to an increased coupling between the subducting and overriding plate, and has caused increased compression in the overriding plate (Graindorge et al. 2004). This might have sealed crustal transfer structures (which in central-northern Ecuador are all trench-parallel) impeding the rapid ascent of magmas from the mantle to the upper crust and forcing them to evolve at greater depth (see also Chiaradia et al. 2004a), thus also modifying the lower crustal thermal structure in a way favorable to mid to lower crust assimilation and mixing processes (Fig. 12).

A major unknown in this model is the debated age of arrival of the Carnegie Ridge at the trench for which estimates range between 1 and 15 Ma. Recent work by Somers et al. (2005) and Amórtegui (2007) as well as ongoing geochronological and geochemical studies of the Tertiary magmatic activity in Ecuador (Schütte et al. 2007) show that adakite-like rocks occur also during the Miocene in the Western Cordillera of Ecuador, intercalated in time with normal calc-alkaline rocks. This could be consistent with the arrival of successive discrete segments of the Carnegie Ridge or other topographic anomalies on top of the subducting oceanic crust throughout the Miocene and until the Quaternary, causing transient compression and the recurrent development of adakite-like signatures.

Conclusions

We have presented new petrographic, geochemical, and isotopic data on lava, cumulate, and crustal xenolith samples from an across-arc transect in Ecuador including five volcanic centers (Pululagua, Pichincha, Ilalo, Chacana, and Sumaco). We observe systematic across-arc geochemical and isotopic changes among the five volcanic centers investigated. First order geochemical differences are source effects, deriving from an isotopically homogeneous mantle progressively less metasomatized by slab fluids as the distance from the trench increases. Differential release of slab fluids also causes decreasing amounts of partial melting from the frontal to the back-arc.

Second order geochemical and isotopic variations occur within each volcanic center: (1) increase of the values of adakitic indices such as Sr/Y and La/Yb with the geochemical evolution of the lavas; (2) significant correlations between magmatic evolution indices and Sr, Nd, Pb isotopes. These features result from similar magmatic processes across the arc, suggesting that magmas did not extensively fractionate plagioclase and evolved within the stability field of clinopyroxene, amphibole ± garnet at least for a part of their history. At the same time, they were assimilating crustal material and/or derivative magmas from previous pulses that had themselves assimilated or melted lower- to mid-crust lithologies, as supported by widespread petrographic evidence for the incorporation and partial assimilation of mafic granulite xenoliths and cumulates (except at Sumaco). Because the isotopic variations within each volcanic center are small but rather well correlated with evolution indices, we conclude that primary melts are assimilating lower- to mid-crustal material and/or its partial melts that are isotopically similar to the primary melts themselves. Such material is probably constituted by Cretaceous oceanic plateau terranes in the Western Cordillera, modified at lower- to mid-crustal levels by the interaction with uprising subduction-related melts since the early Cenozoic. Different and older crust types, modified by Jurassic and Quaternary magmas, could be the assimilants at the main and back-arc volcanic centers. REE modeling requires a maximum of a few percent (<1–2.5%) of garnet as a crystallizing magmatic phase from mantle-derived magmas ponding at lower- to mid-crustal levels and/or as a restitic phase. These magmas are likely to have subsequently mixed and fractionated at different depths of the crustal column.

Isotopic compositions of the least evolved lavas of Ecuador are identical in terms of Sr and Pb isotopes to those of the Tertiary non-adakitic rocks of Ecuador, thus suggesting that the source of magmatism (a mantle wedge enriched by slab fluids) did not change before and after the onset of adakite-like magmatism. Non-adakitic rocks present Eu negative anomalies and a broader variation in Sr isotopic compositions towards radiogenic values, suggesting that these magmas evolved at upper crustal levels through assimilation of crustal lithologies in the plagioclase stability field. In contrast, Quaternary adakite-like rocks display consistently lower radiogenic Sr isotope compositions and no negative Eu anomalies, which indicate assimilation of non-radiogenic mid- to lower-crust mafic material largely outside the plagioclase stability

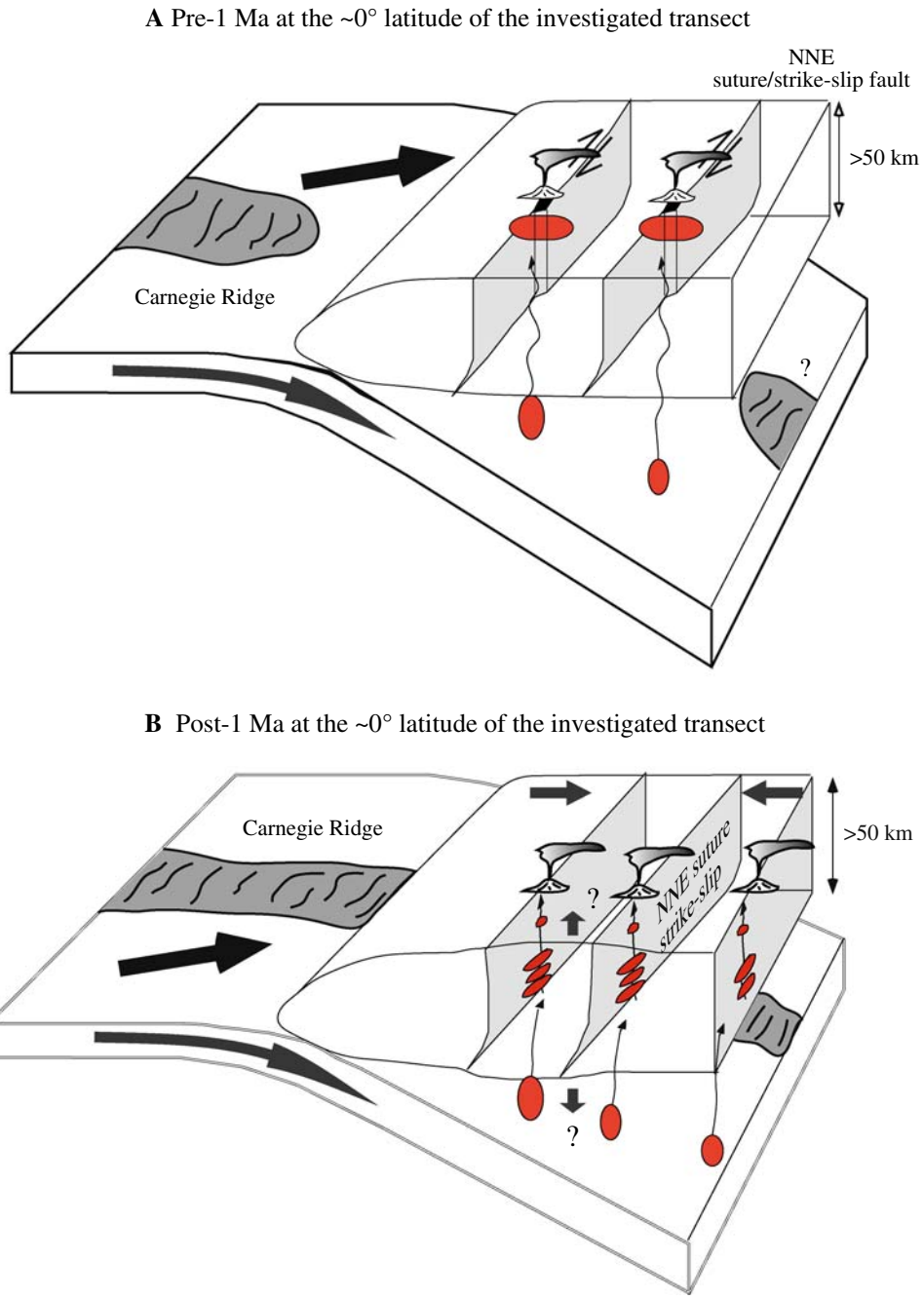

Fig. 12 Cartoons showing hypothetical geodynamic conditions leading to the switch from normal arc to adakite-like signatures in the recent arc magmas of Ecuador at latitudes between 0°30′S and 0°30′N. **a** Before ~1 Ma subduction of "normal" oceanic lithosphere (possibly preceded by a former subduction of a segment of buoyant Carnegie Ridge producing adakite-like signatures in Miocene intrusive rocks of northern Ecuador: Somers et al. 2005; Schütte et al. 2007) is accompanied by melt generation in the mantle wedge and ascent to shallow crustal magma chambers probably related to strike slip faults along the NNE-trending crustal structures (see Fig. 1a), yielding normal arc rock signatures. **b** After ~1 Ma onset of subduction of a section of the buoyant and thick Carnegie Ridge (~20-km thick) causes increased coupling between subducting and overriding plates and possibly shallower angle subduction leading to a broader arc. The increased coupling causes additional compression, sealing of NNE-trending crustal structures and possibly some crustal thickening. As a consequence, mantle-derived melts do not rise readily to shallow crustal levels and evolve at different lower- to mid-crustal levels (deep hot zone) outside the stability field of plagioclase and within that of amphibole ± garnet leading to adakite-like magmas. The water-rich adakite-like magmas that are generated at these depths rise episodically, mixing together, eventually undergoing further fractionation and yielding explosive volcanism typical of the Quaternary Ecuadorian arc

field. We speculate that a change in the depth of magma evolution within the continental crust of northern Ecuador at around 1 Ma might have been related to an increased compressional regime due to the subduction of a segment of the buoyant Carnegie Ridge. Such increased compression could have caused the mantle-derived magmas to evolve at different lower- to mid-crustal levels, whereas previously, under a less compressional regime, magmas could ascend rapidly to upper crustal levels, evolve through assimilation of upper continental crustal rocks and fractionate plagioclase. Arrival of successive discrete segments of the Carnegie Ridge or any other topographic high carried on top of the subducting plate could have been responsible for periods of increased compression and associated adakite-like magmatism since at least the Miocene as supported by the occurrence of several pulses of Miocene adakite-like magmatism along the Western Cordillera of Ecuador (Somers et al. 2005; Schütte et al. 2007).

Acknowledgments We thank Jon Davidson, Sue Kay and Timothy Grove for their constructive reviews, Oliver Jagoutz, Carolina Rodríguez and Daniel Sellés for stimulating discussions and M. Senn as well as F. Capponi for technical help. M.C. acknowledges funding support from the Swiss National Science Foundation (Projects N. 200021-109636 and 200020-117616).

References

Alonso-Perez R (2006) The role of garnet in the evolution of hydrous, calc-alkaline magmas: an experimental study at 0.8–1.5 GPa. PhD thesis, ETH Zurich, p 174

Alonso-Perez R, Müntener O, Ulmer P (2009) Igneous garnet and amphibole fractionation in the roots of island arcs: experimental constraints on H_2O undersaturated andesitic liquids. Contrib Mineral Petrol 157:541–558. doi:10.1007/s00410-008-0351-8

Amórtegui A (2007) Nature et evolution métamorphique des terrains océaniques en Equateur; conséquences possibles sur la genèse des magmas adakitiques. Unpublished PhD Thesis, University Joseph Fourier, Grenoble, France, 179 p

Amórtegui A, Lapierre H, Jaillard E, Martelat J-E, Bosch D, Bussy F, Demant A, Brunet P (2005) Accreted oceanic fragments below the Western Cordillera of Ecuador. Sixth international symposium on Andean geodynamics, ISAG 2005, Barcelona, pp 42–45 (extended abstracts)

Annen C, Blundy JD, Sparks RSJ (2006) The genesis of calc-alkaline intermediate and silicic magmas in deep crustal hot zones. J Petrol 47:505–539. doi:10.1093/petrology/egi084

Arculus RJ, Lapierre H, Jaillard E (1999) Geochemical window into subduction and accretion processes: Raspas metamorphic complex, Ecuador. Geology 27:547–550. doi:10.1130/0091-7613(1999)027<0547:GWISAA>2.3.CO;2

Aspden JA, Litherland M (1992) The geology and Mesozoic collisional history of the Cordillera Real, Ecuador. Tectonophysics 205:187–204. doi:10.1016/0040-1951(92)90426-7

Aspden JA, Harrison SH, Rundle CC (1992) New geochronological control for the tectono-magmatic evolution of the metamorphic basement, Cordillera Real and El Oro Province of Ecuador. J S Am Earth Sci 6:77–96. doi:10.1016/0895-9811(92)90019-U

Atherton MP, Petford N (1993) Generation of sodium rich magmas from newly underplated basaltic crust. Nature 362:144–146. doi:10.1038/362144a0

Barazangi M, Isacks B (1976) Spatial distribution of earthquakes and subduction of the Nazca plate beneath South America. Geology 4:686–692. doi:10.1130/0091-7613(1976)4<686:SDOEAS>2.0.CO;2

Barragan R, Geist D, Hall M, Larsen P, Kurz M (1998) Subduction controls on the compositions of lavas from the Ecuadorian Andes. Earth Planet Sci Lett 154:153–166. doi:10.1016/S0012-821X(97)00141-6

Beate B, Monzier M, Spikings R, Cotten J, Silva J, Bourdon E, Eissen JP (2001) Mio-Pliocene adakite generation related to flat subduction in southern Ecuador: the Quimsacocha volcanic center. Earth Planet Sci Lett 192:561–570. doi:10.1016/S0012-821X(01)00466-6

BGS and CODIGEM (1999) Mapa geologico de la Cordillera Occidental del Ecuador entre 0°–1°S. Mision Britanica, CODIGEM, Quito, Ecuador

BGS and CODIGEM (2001) Mapa geologico de la Cordillera Occidental del Ecuador entre 0°–1° N. Mision Britanica, CODIGEM, Quito, Ecuador

Blundy J, Cashman K, Humphreys M (2006) Magma heating by decompression-driven crystallisation beneath andesite volcanoes. Nature 443:76–80

Bourdon E, Eissen JP, Monzier M, Robin C, Martin H, Cotten J, Hall ML (2002) Adakite-like lavas from Antisana Volcano (Ecuador): evidence for slab melt metasomatism beneath Andean Northern Volcanic Zone. J Petrol 43:199–217

Bourdon E, Eissen JP, Gutscher MA, Monzier M, Hall ML, Cotten J (2003) Magmatic response to early aseismic ridge subduction: the Ecuadorian margin case (South America). Earth Planet Sci Lett 205:123–138

Bryant JA, Yogodzinski GM, Hall ML, Lewicki JL, Bailey DG (2006) Geochemical constraints on the origin of volcanic rocks from the Andean Northern Volcanic Zone, Ecuador. J Petrol 47:1147–1175

Calvache ML, Williams SN (1997) Geochemistry and petrology of the Galeras Volcanic Complex, Colombia. J Volcanol Geotherm Res 77:21–38

Castillo PR, Janney PE, Solidum RU (1999) Petrology and geochemistry of Camiguin Island, southern Philippines: insights to the source of adakites and other lavas in a complex arc setting. Contrib Mineral Petrol 134:33–51

Chiaradia M, Fontboté L (2001) Radiogenic lead signatures in Au-rich VHMS ores and associated volcanic rocks of the Early Tertiary Macuchi island arc (Western Cordillera of Ecuador). Econ Geol 96:1361–1378

Chiaradia M, Fontboté L, Beate B (2004a) Cenozoic continental arc magmatism and associated mineralization in Ecuador. Mineral Dep 39:204–222

Chiaradia M, Fontboté L, Paladines A (2004b) Metal sources in mineral deposits and crustal rocks of Ecuador (1°N–4°S): a lead isotope synthesis. Econ Geol 99:1085–1106

Chiaradia M, Vallance J, Fontboté L, Stein H, Schaltegger U, Coder J, Richards J, Villeneuve M, Gendall I (2009) U–Pb, Re–Os and $^{40}Ar/^{39}Ar$ geochronology of the Nambija Au skarn and Pangui porphyry–Cu deposits, Ecuador: implications for the Jurassic metallogenic belt of the Northern Andes. Miner Depos. doi:10.1007/s00126-008-0210-6

Class C, Miller DM, Goldstein SL, Langmuir CH (2000) Distinguishing melt and fluid subduction components in Umnak Volcanics, Aleutian Arc. Geochem Geophys Geosyst 1999GC000010

Condie KC (2005) TTGs and adakites: are they both slab melts? Lithos 80:33–44

Cooke DR, Hollings P, Walshe JL (2005) Giant porphyry deposits: characteristics, distribution, and tectonic controls. Econ Geol 100:801–818

Davidson JP, de Silva SL (1995) Cenozoic magmatism of the Bolivian Altiplano. Contrib Mineral Petrol 119:387–408

Davidson J, Turner S, Handley H, Macpherson C, Dosseto A (2007) Amphibole "sponge" in arc crust? Geology 35:787–790

Defant MJ, Drummond MS (1990) Derivation of some modern arc magmas by melting of young subducted lithosphere. Nature 347:662–665

DePaolo DJ (1981) Trace element and isotopic effects of combined wallrock assimilation and fractional crystallization. Earth Planet Sci Lett 53:189–202

Dickinson WR (1975) Potash–depth (K–h) relations in continental margin and intra-oceanic magmatic arcs. Geology 3:53–56

Droux A, Delaloye M (1996) Petrography and geochemistry of Plio-Quaternary calc-alkaline volcanoes of southwestern Colombia. J S Am Earth Sci 9:27–41

Dufek J, Bergantz GW (2005) Lower crustal magma genesis and preservation: a stochastic framework for the evaluation of basalt–crust interaction. J Petrol 46:2167–2195

Dungan M, Davidson JP (2004) Partial assimilative recycling of the mafic plutonic roots of arc volcanoes: an example from the Chilean Andes. Geology 32:773–776

Dungan MA, Wulff A, Thompson RA (2001) Eruptive stratigraphy of the Tatara-San Pedro complex, 36°S, Southern Volcanic Zone, Chilean Andes: reconstruction methodology and implications for magma evolution at long-lived arc volcanic centers. J Petrol 42:555–626

Edwards CMH, Menzies MA, Thirlwall MF, Morros JD, Leeman WP, Harmon RS (1994) The transition to potassic alkaline volcanism in islands arcs: the Ringgit–Beser complex, East Java, Indonesia. J Petrol 35:1557–1595

Ego F, Sébrier M, Lavenu A, Yepes H, Egues A (1996) Quaternary state of stress in the Northern Andes and the restraining bend model for the Ecuadorian Andes. Tectonophysics 259:101–116

Engdahl ER, van der Hilst RD, Buland RP (1988) Global teleseismic earthquake relocation with improved travel times and procedures for depth determination. Bull Seism Soc Am 88:722–743

Feininger T (1987) Allochthonous terranes in the Andes of Ecuador and northwestern Peru. Can J Earth Sci 24:266–278

Feininger T, Seguin MK (1983) Bouguer gravity anomaly field and inferred crustal structure of continental Ecuador. Geology 11:40–44

Fornari M, Monzier M, Samaniego P, Robin C, Beate B, Bourdon E, Eissen JP, Féraud G (2004) Ar–Ar dating of active Quaternary Pichincha volcano, Quito, Ecuador. Geophysical Research Abstracts 6, 02442

Garrido CG, Bodinier JL (2005) Intracrustal Nb/Ta fractionation in island arcs due to dehydration melting of hornblende-bearing plutonics: evidence from the Kohistan paleo-island arc complex (N. Pakistan). Geophysical Research Abstracts vol 7, 06350

Garrison JM, Davidson JP (2003) Dubious case for slab melting in the Northern volcanic zone of the Andes. Geology 31:565–568

Garrison JM, Davidson J, Reid M, Turner S (2006) Source versus differentiation controls on U-series disequilibria: insights from Cotopaxi Volcano, Ecuador. Earth Planet Sci Lett 244:548–565

Graindorge D, Calahorrano A, Charvis P, Collot JY, Bethoux N (2004) Deep structure of the Ecuador convergent margin and the Carnegie Ridge, possible consequences on great earthquakes recurrence interval. Geophysical Res Lett 31. doi:10.1029/2003GL018803

Green TH (1972) Crystallization of calc-alkaline andesite under controlled high-pressure hydrous conditions. Contrib Mineral Petrol 34:150–166

Green TH (1982) Anatexis of mafic crust and high pressure crystallization of andesite. In: Thorpe RS (ed) Orogenic Andesites and related rocks. Wiley, New York, pp 465–487

Grove TL, Chatterjee N, Parman SW, Médard E (2006) The influence of H_2O on mantle wedge melting. Earth Planet Sci Lett 249:74–89

Guillier B, Chatelain JL, Jaillard E, Yepes H, Poupinet G, Fels JF (2001) Seismological evidence on the geometry of the orogenic system in central–northern Ecuador (South America). Geophys Res Lett 28:3749–3752

Gutscher MA, Malavieille J, Lallemand S, Collot JY (1999) Tectonic segmentation of the North Andean margin: impact of the Carnegie Ridge collision. Earth Planet Sci Lett 168:255–270

Hacker BR, Peacock SM, Abers GA, Holloway SD (2003) Subduction factory 2. Are intermediate-depth earthquakes in subducting slabs linked to metamorphic dehydration reactions? J Geophys Res 108, n. B1, 2030, doi:10.1029/2001JB001129

Harmon RS, Barreiro B, Moorbath S, Hoefs J, Francis PW, Thorpe RS, Deruelle B, McHugh J, Viglino JA (1984) Regional O-, Sr-, and Pb-isotope relationships in the late Cenozoic calc-alkaline lavas of the Andean Cordillera. J Geol Soc Lond 141:803–822

Hidalgo S, Monzier M, Martin H, Chazot G, Eissen JP, Cotton J (2007) Adakitic magmas in the Ecuadorian Volcanic Front: petrogenesis of the Iliniza Volcanic Complex (Ecuador). J Volcanol Geotherm Res 159:366–392

Hildreth W, Moorbath S (1988) Crustal contributions to arc magmatism in the Andes of central Chile. Contrib Mineral Petrol 98:455–489

Hoffer G, Eissen JP, Beate B, Bourdon E, Fornari M, Cotton J (2008) Geochemical and petrological constraints on rear-arc magma genesis processes in Ecuador: the Puyo cones and Mera lavas volcanic formations. J Volcanol Geotherm Res 176:107–118

Hughes RA, Pilatasig LF (2002) Cretaceous and Tertiary terrane accretion in the Cordillera Occidental of the Andes of Ecuador. Tectonophysics 345:29–48

Irving AJ, Frey FA (1976) Effect of composition on partitioning of rare-earth elements, Hf, Sc and Co between Garnet and Liquid: experimental and natural evidence. EOS Trans Am Geophys Union 57:339

Jaillard E, Soler P, Carlier G, Mourier T (1990) Geodynamic evolution of the northern and central Andes during early-to-middle Mesozoic times: a Tethyan model. J Geol Soc Lond 147:1009–1022

Jaillard E, Benítez S, Mascle GH (1997) Les déformations paléogenes de la zone d'avant-arc sud-équatorienne en relation avec l'évolution géodynamique. Bull Soc Geol Fr 168:403–412

James DE (1982) A combined O, Sr, Nd, and Pb isotopic and trace element study of crustal contamination in central Andean lavas, I. Local geochemical variations. Earth Planet Sci Lett 57:47–62

Kamber BS, Ewart A, Collerson KD, Bruce MC, McDonald GD (2002) Fluid-mobile trace element constraints on the role of slab melting and implications for Archaean crustal growth models. Contrib Mineral Petrol 144:38–56

Kay RW (1978) Aleutian magnesian andesites: melts from subducted Pacific ocean crust. J Volcanol Geotherm Res 4:117–132

Kay SM, Mpodozis C (2001) Central Andean ore deposits linked to evolving shallow subduction systems and thickening crust. GSA Today 11:4–9

Kay S, Maksaev V, Mpodozis C, Moscoso R, Nasi C (1987) Probing the evolving Andean lithosphere: middle to late Tertiary magmatic rocks in Chile over the modern zone of subhorizontal subduction (29 31.5°S). J Geophys Res 92:6173–6189

Kay SM, Mpodozis C, Ramos VA, Munizaga E (1991) Magma source variations for mid to late Tertiary volcanic rocks erupted over a shallowing subduction zone and through a thickening crust in the Main Andean Cordillera (28–33°S). In: Harmon RS, Rapel C

(eds) Andean magmatism and its tectonic setting, Geol Soc Am Spec Pap 265, pp 113–137
Kay SM, Ramos VA, Marquez YM (1993) Evidence in Cerro Pampa volcanic rocks for slab-melting prior to ridge–trench collision in southern South America. J Geol 101:703–714
Kay SM, Mpodozis C, Coira B (1999) Magmatism, tectonism, and mineral deposits of the Central Andes (22°–33°S latitude. In: Skinner B (ed) Geology and ore deposits of the Central Andes, Society of Economic Geology Special Publication 7, pp 27–59
Kelemen PB (1995) Genesis of high Mg# andesites and the continental crust. Contrib Mineral Petrol 120:1–19
Kelemen PB, Hanghoj K, Greene AR (2004) One view of the geochemistry of subduction-related magmatic arcs, with an emphasis on primitive andesite and lower crust. In: Holland HD, Turekian KK (eds) Treatise on geochemistry. Elsevier, Amsterdam, pp 593–659
Kerr AC, Tarney J (2005) Tectonic evolution of the Caribbean and northwestern South America: the case for accretion of two Late Cretaceous oceanic plateaus. Geology 33:269–272
Kerr AC, Marriner GF, Tarney J, Nivia A, Saunders AD, Thirlwall MF (1997) Cretaceous basaltic terranes in western Colombia; elemental, chronological and Sr–Nd isotopic constraints on petrogenesis. J Petrol 38:677–702
Kessel R, Ulmer P, Pettke T, Schmidt M, Thompson AB (2005) The water basalt system at 4 to 6 GPa: phase relations and second critical endpoint in a K-free eclogite at 700 to 1400°C. Earth Planet Sci Lett 237:873–892
Kilian R, Hegner E, Fortier S, Satir M (1995) Magma evolution within the accretionary mafic basement of Quaternary Chimborazo and associated volcanos (Western Ecuador). Rev Geol Chile 22:203–208
Kincaid C, Griffiths RW (2004) Variability in flow and temperatures within mantle subduction zones. Geochem Geophys Geosyst 5:Q06002. doi:10.1029/2003GC000666
Lee C-TA, Cheng X, Horodyskyj U (2006) The development and refinement of continental arcs by primary basaltic magmatism, garnet pyroxenite accumulation, basaltic recharge and delamination: insights from the Sierra Nevada. Contrib Mineral Petrol 151:222–242
Litherland M, Aspden JA, Jemielita RA (1994) The metamorphic belts of Ecuador. British Geological Survey, Keyworth, 147 p
Lonsdale P (1978) Ecuadorian subduction system. AAPG Bull 62(12):2454–2477
Lonsdale P, Klitgord KD (1978) Structure and tectonic history of the eastern Panama basin. Geol Soc Am Bull 89:1–9
Macpherson CG, Dreher ST, Thirlwall MF (2006) Adakites without slab melting: high pressure differentiation of island arc magma, Mindanao, The Philippines. Earth Planet Sci Lett 243:581–593
Mamberti M, Lapierre H, Bosch D, Jaillard E, Ethien R, Hernandez J, Polvé M (2003) Accreted fragments of the Late Cretaceous Caribbean–Colombian Plateau in Ecuador. Lithos 66:173–199
Martin H (1999) Adakitic magmas: modern analogues of Archaean granitoids. Lithos 46:411–429
Martin H, Smithies RH, Rapp R, Moyen J-F, Champion D (2005) An overview of adakite, tonalite–trondhjemite–granodiorite (TTG), and sanukitoid: relationships and some implications for crustal evolution. Lithos 79:1–24
Mashima H (2004) Time scale of magma mixing between basalt and dacite estimated for the Saga–Futagoyama volcanic rocks in northwest Kyushu, southwest Japan. J Volcanol Geotherm Res 131:333–349
Matile L, Thompson AB, Ulmer P (2000) A fractionation model for hydrous calc-alkaline plutons and the heat budget during fractional crystallization and assimilation. In: Bagdassarov N et al (eds) Physics and chemistry of partially molten rocks. Kluwer, Dordrecht, pp 179–208
Megard F (1989) The evolution of the Pacific Ocean margin in South America north of Arica elbow (18 S). In: Ben Avraham Z (ed) Oxford monographs on geology and geophysics no. 8. Oxford University Press, New York, pp 208–230
Monzier M, Robin C, Samaniego P, Hall ML, Cotten J, Mothes P, Arnaud N (1999) Sangay Volcano, Ecuador: structural development, present activity and petrology. J Volcanol Geotherm Res 90:49–79
Müntener O, Ulmer P (2006) Experimentally derived high-pressure cumulates from hydrous arc magmas and consequences for the seismic velocity structure of lower arc crust. Geophys Res Lett 33:L21308. doi:10.1029/2006GL027629
Müntener O, Kelemen PB, Grove TL (2001) The role of H_2O during crystallization of primitive arc magmas under uppermost mantle conditions and genesis of igneous pyroxenites: an experimental study. Contrib Mineral Petrol 141:643–658
Noble SR, Aspden JA, Jemielita RA (1997) Northern Andean crustal evolution: new U–Pb geochronological constraints from Ecuador. Geol Soc Am Bull 109:789–798
Peccerillo A, Taylor SR (1976) Geochemistry of Eocene calc-alkaline volcanic rocks from the Kastamonu area, Northern Turkey. Contrib Mineral Petrol 58:63–81
Pedoja K, Dumont JF, Lamothe M, Ortlieb L, Collot JY, Ghaleb B, Auclair M, Alvarez V, Labrousseb B (2006) Plio-Quaternary uplift of the Manta Peninsula and La Plata Island and the subduction of the Carnegie Ridge, central coast of Ecuador. J S Am Earth Sci 22:1–21
Pennington WD (1981) Subduction of the eastern Panama basin and seismotectonics of northwestern South America. J Geophys Res 86(B 11):10753–10770
Petford N, Gallagher K (2001) Partial melting of mafic (amphibolitic) lower crust by periodic influx of basaltic magma. Earth Planet Sci Lett 193:483–499
Pilet S, Baker MB, Stolper EM (2008) Metasomatized lithosphere and the origin of alkaline lavas. Science 320:916–919
Pratt WT, Duque P, Miguel P (2005) An autochthonous geological model for the eastern Andes of Ecuador. Tectonophysics 399:251–278
Prévot R, Chatelain J-L, Guillier B, Yepes H (1996) Tomographie des Andes Equatoriennes: évidence d'une continuité des Andes Centrales. Comp Rend Acad Sci, Série II. Sciences de la Terre et des Planètes 323:833–840
Reynaud C, Jaillard E, Lapierre H (1999) Oceanic plateau and island arcs of SW Ecuador: their place in the geodynamic evolution of northwestern South America. Tectonophysics 307:235–254
Rodríguez C, Sellés D, Dungan M, Langmuir C, Leeman W (2007) Adakitic Dacites formed by intracrustal crystal fractionation of water-rich parent magmas at Nevado de Longaví Volcano (36.2°S; Andean Southern Volcanic Zone, Central Chile). J Petrol 48:2033–2061
Rutherford MJ, Hill PM (1993) Magma ascent rates from amphibole breakdown: an experimental study applied to the 1980–1986 Mount St Helens eruptions. J Geophys Res 98:19,667–19685
Ryan JG, Morris J, Tera F, Leeman WP, Tsvetkov A (1995) Cross-arc geochemical variations in the Kurile arc as a function of slab depth. Science 270:625–627
Sage F, Collot J-Y, Ranero CR (2006) Interplate patchiness and subduction–erosion mechanisms: evidence from depth-migrated seismic images at the central Ecuador convergent margin. Geology 34:997–1000
Samaniego P, Martin H, Robin C, Monzier M (2002) Transition from calc-alkalic to adakitic magmatism at Cayambe volcano, Ecuador: insights into slab melts and mantle wedge interactions. Geology 30:967–970
Samaniego P, Martin H, Monzier M, Robin C, Fornari M, Eissen JP, Cotten J (2005) Temporal evolution of magmatism in the

Northern Volcanic Zone of the Andes: the geology and petrology of Cayambe Volcanic Complex (Ecuador). J Petrol 46:2225–2252

Sato H (1975) Diffusion coronas around quartz xenocrysts in andesite and basalt from Tertiary Volcanic Region in Northeastern Shikoku, Japan. Contrib Mineral Petrol 50:49–64

Schütte P, Chiaradia M, Beate B (2007) Geochronology and geochemistry of tertiary intrusions associated with porphyry-type deposits in Ecuador. Program with abstracts, ores and orogenesis symposium, 24–29 September 2007, Tucson, Arizona, p 182

Smithies RH (2000) The Archaean tonalite–trondhjemite–granodiorite (TTG) series is not an analogue of Cenozoic adakite. Earth Planet Sci Lett 182:115–125

Somers C, Amórtegui A, Lapierre H, Jaillard E, Bussy F, Brunet P (2005) Miocene adakitic intrusions in the Western Cordillera of Ecuador. Sixth international symposium on Andean geodynamics, ISAG 2005, Barcelona, pp 679–680 (extended abstracts)

Spikings RA, Winkler W, Seward D, Handler R (2001) Along-strike variations in the thermal and tectonic response of the continental Ecuadorian Andes to the collision with heterogeneous oceanic crust. Earth Planet Sci Lett 186:57–73

Spikings RA, Winkler W, Hughes RA, Handler R (2005) Thermochronology of allochthonous terranes in Ecuador: unravelling the accretionary and post-accretionary history of the Northern Andes. Tectonophysics 399:195–220

Stern CR, Kilian R (1996) Role of the subducted slab, mantle wedge and continental crust in the generation of adakites from the Andean Austral Volcanic Zone. Contrib Mineral Petrol 123:263–281

Stimac JA, Pearce TH (1992) Textural evidence of mafic–felsic magma interaction in dacite lavas, Clear Lake. Am Mineral 77:795–809

Stolper EM, Newman S (1994) The role of water in the petrogenesis of the Marian trough magmas. Earth Planet Sci Lett 121:293–325

Storkey AC, Hermann J, Hand M, Buick IS (2005) Using in situ trace-element determinations to monitor partial-melting processes in metabasites. J Petrol 46:1283–1308

Sun SS, McDonough WF (1989) Chemical and isotopic systematics of oceanic basalts: implications for mantle composition and processes. In: Saunders AD, Norry MJ (eds) Magmatism in the Ocean Basins. Geological Society, London, Special Publications 42: 313–346

Tatsumi Y, Koyaguchi K (1989) An absarokite from a phlogopite lherzolite source. Contrib Mineral Petrol 102:34–40

Thieblemont D, Stein G, Lescuyer JL (1997) Gisements épithermaux et porphyriques: la connexion adakite = epithermal and porphyry deposits: the adakite connection. Comptes Rendus Acad Sci, Série 2, Sci Terre Plan 325: 103–109

Thorpe RS, Francis PW, O'Callaghan L (1983) Relative roles of source composition, fractional crystallization and crustal contamination in the petrogenesis of Andean volcanic rocks. Philos Trans R Soc Lond Ser A 310:675–692

Tiepolo M, Vannucci R, Oberti R, Foley S, Bottazzi P, Zanetti A (2000) Nb and Ta incorporation and fractionation in titanian pargasite and kaersutite: crystal-chemical constraints and implications for natural systems. Earth Planet Sci Lett 176:185–201

Vallejo C (2007) Evolution of the Western Cordillera in the Andes of Ecuador (Late Cretaceous–Paleogene). Unpublished PhD Thesis, ETHZ, Zürich, Switzerland, 208 p

Vallejo C, Spikings RA, Luzieux L, Winkler W, Chew D, Page L (2006) The early interaction between the Caribbean Plateau and the NW South American Plate. Terra Nova 18:264–269

van Keken PE, Kiefer B, Peacock SM (2002) High-resolution models of subduction zones: implications for mineral dehydration reactions and the transport of water into the deep mantle. Geochem Geophys Geosyst 3:1056. doi:10.1029/2001GC000256

Vanek J, Vankova V, Hanus V (1994) Geochemical zonation of volcanic rocks and deep structure of Ecuador and southern Colombia. J S Am Earth Sci 7:57–67

Villagomez D, Eguez A, Winkler W, Spikings R (2002) Plio-Quaternary sedimentary and tectonic evolution of the central Inter-andean Valley in Ecuador. 4th International Symposium on Andean Geodynamics, ISAG 2002, Tolouse, pp 689–692 (extended abstracts)

Weber MBI, Tarney J, Kempton PD, Kent RW (2002) Crustal make-up of the northern Andes: evidence based on deep crustal xenolith suites, Mercaderes, SW Colombia. Tectonophysics 345:49–82

White WM, McBirney AR, Duncan RA (1993) Petrology and geochemistry of the Galapagos Islands: portrait of a pathological mantle plume. J Geophys Res 98:19533–19563

Yogodzinski GM, Kay RW, Volynets ON, Koloskov AV, Kay SM (1995) Magnesian andesite in the western Aleutian Komandorsky region: implications for slab melting and processes in the mantle wedge. Geol Soc Am Bull 107:505–519

Zartman RE, Doe BR (1981) Plumbotectonics—the model. Tectonophysics 75:135–162

Zindler A, Hart S (1986) Chemical geodynamics. Ann Rev Earth Planet Sci 14:493–571